

Michelle Singleton
Department of Anatomy,
Midwestern University, 555
31st Street, Downers Grove,
Illinois 60515, U.S.A.
E-mail:
msingl@midwestern.edu

Received 10 January 2001
Revision received
26 October 2001 and
accepted 12 December 2001

Keywords: Papionini,
mangabey diphyly, cranial
homoplasy, allometry,
geometric morphometrics.

Patterns of cranial shape variation in the Papionini (Primates: Cercopithecinae)


Traditional classifications of the Old World monkey tribe Papionini (Primates: Cercopithecinae) recognized the mangabey genera *Cercocebus* and *Lophocebus* as sister taxa. However, molecular studies have consistently found the mangabeys to be diphyletic, with *Cercocebus* and *Mandrillus* forming a clade to the exclusion of all other papionins. Recent studies have identified cranial and postcranial features which distinguish the *Cercocebus*–*Mandrillus* clade, however the detailed similarities in cranial shape between the mangabey genera are more difficult to reconcile with the molecular evidence. Given the large size differential between members of the papionin molecular clades, it has frequently been suggested that allometric effects account for homoplasy in papionin cranial form. A combination of geometric morphometric, bivariate, and multivariate methods was used to evaluate the hypothesis that allometric scaling contributes to craniofacial similarities between like-sized papionin taxa. Patterns of allometric and size-independent cranial shape variation were subsequently described and related to known papionin phylogenetic relationships and patterns of development.

Results confirm that allometric scaling of craniofacial shape characterized by positive facial allometry and negative neurocranial allometry is present across adult papionins. Pairwise comparisons of regression lines among genera revealed considerable homogeneity of scaling within the Papionini, however statistically significant differences in regression lines also were noted. In particular, *Cercocebus* and *Lophocebus* exhibit a shared slope and significant vertical displacement of their allometric lines relative to other papionins. These findings give no support to narrowly construed hypotheses of uniquely shared patterns of allometric scaling, either between sister taxa or across all papionins. However, more general allometric trends do appear to account for a substantial proportion of papionin cranial shape variation, most notably in those features which have influenced traditional morphological phylogenies. Examination of size-uncorrelated shape variation gives no clear support to molecular phylogenies, but underscores the absence of morphometric similarities between the mangabey genera when size effects are controlled. Patterns of allometric and size-uncorrelated shape variation indicate conservatism of cranial form in non-*Theropithecus* papionins, and suggest that *Papio* represents the primitive morphometric pattern for the African papionins. *Lophocebus* exhibits a divergent morphometric pattern, clearly distinguishable from other papionins, most notably *Cercocebus*. These results clarify patterns of cranial shape variation among the extant Papionini and lay the groundwork for studies of related fossil taxa.

© 2002 Elsevier Science Ltd

Journal of Human Evolution (2002) 42, 547–578

doi:10.1006/jhev.2001.0539

Available online at <http://www.idealibrary.com> on 

Introduction

The Old World monkey tribe Papionini (Primates: Cercopithecinae) comprises a monophyletic group of six extant genera. While *Macaca* is widely acknowledged as representing the sister taxon to the African papionins (Strasser & Delson, 1987; Morales & Melnick, 1998), relationships among the latter taxa have been a source of controversy. Traditional classifications recognized the mangabey genera *Cercocebus* and *Lophocebus* as sister taxa and frequently accorded them congeneric status on the basis of shared morphological traits (Thorington & Groves, 1970; Szalay & Delson, 1979). However, molecular studies have consistently found the mangabeys to be diphyletic, with *Cercocebus* and *Mandrillus* forming a clade to the exclusion of all other papionins (Harris, 2000). Recent studies have identified a number of features which distinguish the *Cercocebus*–*Mandrillus* clade (Fleagle & McGraw, 1999; Groves, 2000); however the detailed similarities in cranial shape between the mangabey genera have yet to be reconciled with molecular phylogenies. Because of the large size differential between members of the papionin molecular clades, it frequently has been suggested that allometric effects might account for homoplasies in papionin cranial shape (Shah & Leigh, 1995; Lockwood & Fleagle, 1999; Harris, 2000; Ravosa & Profant, 2000).

In an effort to circumvent certain limitations of traditional allometric studies, a geometric morphometric study of papionin craniofacial morphology was undertaken. A combination of geometric morphometric, bivariate, and multivariate techniques was applied in order to identify multivariate scaling patterns not discernable by conventional bivariate regression analysis. The objectives of this study were twofold. The first was to evaluate the supposition that homoplasy in papionin craniofacial shape is attributable to shared patterns of allometric scaling,

either within individual clades or across all papionins. The second was to describe patterns of allometric and residual (size-uncorrelated) cranial shape variation and interpret these patterns in the light of prior studies of papionin ontogeny and phylogeny.

Background

The Old World monkey tribe Papionini Burnett, 1828 (Primates, Cercopithecinae) encompasses six extant genera: *Macaca*, the macaques; *Cercocebus* and *Lophocebus*, the mangabeys; *Mandrillus*, including mandrills and drills; *Papio*, the savannah baboons; and *Theropithecus*, the gelada baboon. The papionins have long been recognized as a monophyletic group on the basis of shared traits including relatively flaring molars, broad nasal apertures, relatively long faces, a tendency toward terrestriality, and a diploid chromosome number of 42 (Kuhn, 1967; Hill, 1974; Delson, 1975a,b; Szalay & Delson, 1979; Dutrillaux *et al.*, 1982; Strasser & Delson, 1987). *Macaca*, which lacks well-developed maxillary and mandibular facial fossae and is thought to retain a number of primitive cercopithecine morphological features, is considered the sister taxon to the African papionins (Szalay & Delson, 1979; Strasser & Delson, 1987; Morales & Melnick, 1998). This relationship is confirmed by an array of molecular evidence including immunological distances, protein polymorphisms, DNA–DNA hybridization, amino acid sequences, and nuclear and mitochondrial genetic studies (Disotell, 1994; van der Kuyl *et al.*, 1995; Harris & Disotell, 1998; Harris, 2000).

The resolution of phylogenetic relationships among the African papionins has been more problematic. The mangabeys were often classified in a single genus, *Cercocebus*, on the basis of shared morphological features including moderate body size,

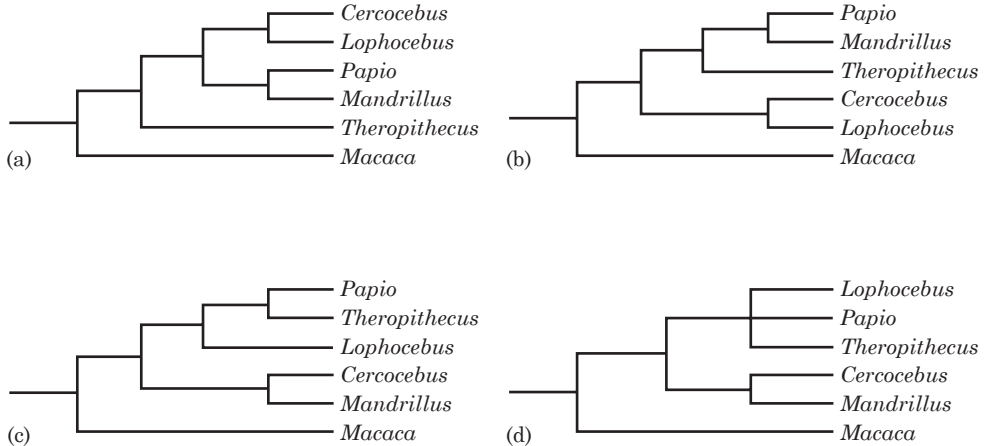


Figure 1. Cladograms depicting alternate hypotheses of phylogenetic relationships among the Papionini. Traditional phylogenies exemplified by (a) Strasser & Delson (1987) and (b) Delson & Dean (1993) recognized the mangabey genera *Cercocebus* and *Lophocebus* as sister taxa. Molecular phylogenies, including (c) Disotell (1994) and (d) Harris & Disotell (1998), reconstruct mangabeys as diphyletic, with *Cercocebus* most closely related to *Mandrillus*.

relatively short muzzles, excavated sub-orbital fossae, and retention of a long tail (Thorington & Groves, 1970; Hill, 1974; Szalay & Delson, 1979). However, consistent morphological and behavioral differences were noted between two recognized species groups—a semi-terrestrial *torquatus-galeritus* group and a highly arboreal *albigena-atterimus* group (Schwarz, 1928; Jones & Sabater Pi, 1968; Hill, 1974)—which were sometimes accorded subgeneric status (Szalay & Delson, 1979). Groves (1978) resurrected the genus *Lophocebus* Palmer, 1903, to receive the *albigena-atterimus* species group, which he diagnosed on the basis of skeletal, behavioral, and reproductive traits. Still, *Cercocebus* and *Lophocebus* were generally considered closely related (Kuhn, 1967; Szalay & Delson, 1979; Strasser & Delson, 1987), and many phylogenetic hypotheses reconstructed the mangabeys as sister taxa to the exclusion of the remaining African papionins [Figure 1(a), (b)].

By contrast, molecular studies have consistently indicated that mangabeys are diphyletic [Figure 1(c), (d)]. Beginning with

the earliest protein electrophoresis and immunological studies (Barnicott & Hewett-Emmett, 1972; Cronin & Sarich, 1976; Hewett-Emmett *et al.*, 1976), analyses of chromosome structure, amino acid sequences, mitochondrial and nuclear DNA have all linked *Cercocebus* and *Mandrillus* to the exclusion of *Lophocebus*, *Papio* and *Theropithecus* (Dutrilleaux *et al.*, 1979, 1982; Disotell *et al.*, 1992; Disotell, 1994; van der Kuyl *et al.*, 1995; Harris & Disotell, 1998; Page *et al.*, 1999; Harris, 2000). Cladistic relationships among the latter taxa are somewhat less clear. Trees based on immunological distances and certain DNA sequences (CO II and γ -globin) support a *Papio-Theropithecus* sister relationship (Cronin & Sarich, 1976; Disotell, 1994; Page *et al.*, 1999). Three of the four nuclear sequences ($\psi\eta$ - δ globin intergenic region; α 1,3 GT; IRBP) analyzed by Harris & Disotell (1998) support a *Papio-Lophocebus* sister relationship. In a recent synthesis of published molecular data, Harris (2000) found that both molecular consensus and total molecular evidence trees supported the *Lophocebus-Papio* clade,

although a *Lophocebus*–*Papio*–*Theropithecus* trichotomy could not be rejected statistically. This point of uncertainty notwithstanding, mangabey diphyly appears well supported.

The obvious discrepancy between molecular and morphological classifications of the papionins has led to renewed interest in the behavior, ecology, reproductive biology, and especially the comparative morphology of this group. Nakatsukasa (1994, 1996) identified a number of postcranial features distinguishing *Cercocebus* from *Lophocebus*, and Fleagle & McGraw (1999) established that *Cercocebus* more closely resembles *Mandrillus* in these same features. They also noted the presence of enlarged fourth premolars in this clade in comparison with *Papio* and *Lophocebus*. Based on outgroup comparisons with *Macaca nemestrina*, they judged the postcranial traits primitive and the dental dimensions derived, and they attributed this suite of features to a shared ecological adaptation, namely terrestrial foraging and hard object feeding in a tropical forest milieu (Fleagle & McGraw, 1999). More recently, additional qualitative cranial features have been put forward as potential synapomorphies of a *Cercocebus*–*Mandrillus* clade (McGraw & Fleagle, 2000; Groves, 2000).

The marked similarities in cranial shape and proportion which distinguish *Cercocebus* and *Lophocebus* from other African papionins have proven less tractable to analysis, giving rise to evolutionary scenarios invoking various combinations of primitive retention and parallel evolution within the two African molecular clades. Based on outgroup comparisons, it has been suggested that the moderate facial length seen in mangabeys—like moderate body size and the presence of a long tail—is primitive for all papionins (Disotell, 1994; Harris & Disotell, 1998; Harris, 2000). This would imply that *Papio* and *Mandrillus* experienced parallel increases in facial length. However,

Groves (1978) and Kingdon (1997) have proposed that long faces are primitive for African papionins. In this scenario, the *Cercocebus* and *Lophocebus* lineages would have experienced parallel reductions in facial length, with the excavated suborbital fossae found in these taxa perhaps resulting from this secondary facial shortening (Harris & Disotell, 1998; Harris, 2000).

Allometric scaling of cranial proportions is well-documented within the Papionini. Freedman (1962) showed that adult facial length scales positively relative to calvaria length both between males and females and across (sub)species of *Papio*. He subsequently related differences in cranial proportions among *Papio* varieties to clinal trends in body size (Freedman, 1963). Ontogenetic studies of macaques have consistently shown that males and females follow a common trajectory characterized by positive facial allometry, negative allometry of neurocranial dimensions, and dorsal rotation of the maxilla and palate, with sexual dimorphism between adult cranial form resulting from male hypermorphosis (MacNamara *et al.*, 1976; Bookstein, 1985; Cochard, 1985; Cheverud & Richtsmeier, 1986). Comparative developmental studies have found *Papio* and *Macaca* to have similar craniofacial growth rates and a common ontogenetic trajectory characterized by progressive increase in cranial base angle, relatively rapid forward growth of the muzzle, proportional increase in lower facial height, and decelerating neurocranial growth (Swindler & Sirianni, 1973; Swindler *et al.*, 1973). Thus, many observed differences in adult cranial morphologies of macaques and baboons are construed as allometric consequences of *Papio*'s larger absolute body size.

It has frequently been suggested that allometric effects might also account for homoplasies in mangabey cranial shape (Shah & Leigh, 1995; Lockwood & Fleagle, 1999; Harris, 2000; Ravosa & Profant,

2000). Comparing adult male body weights, *Mandrillus sphinx* averages 34 kg; *M. leucophaeus*, 20 kg; and *Papio hamadryas* subspecies range from a mean weight of 16 kg (*P. h. kindae*) to 31 kg (*P. h. anubis*) (Delson *et al.*, 2000). By comparison, males of the larger *Cercocebus* varieties average only 12 kg (*C. torquatus torquatus*); and *Lophocebus* males average no more than 9 kg (*L. albigena zenkeri*) (Delson *et al.*, 2000). Given this marked size difference, it is highly plausible that craniofacial similarities between like-sized members of disparate papionin clades can be explained in terms of interspecific allometric scaling. In particular, it has been suggested that ontogenetic scaling—whereby adults of papionin sister taxa occupy different points along a shared growth trajectory (Shea, 1985)—may be a major factor in mangabey cranial homoplasy (Shah & Leigh, 1995). Shah & Leigh's (1995) initial efforts to test the hypothesis of ontogenetic scaling within the *Cercocebus*–*Mandrillus* clade were inconclusive. They found that *Mandrillus* and *Cercocebus* shared a common ontogenetic trajectory for neurocranial dimensions, but facial growth in *Mandrillus* more closely resembled that of *Papio*. The authors concluded that scaling patterns among these taxa were complex, and that global ontogenetic scaling could not adequately account for differences in cranial shape between *Cercocebus* and *Mandrillus*.

Minor variations in scaling patterns of individual linear dimensions within and between cranial regions can unnecessarily complicate interspecific allometric comparisons. By design, linear measures reduce complex spatial relationships to unidimensional values lacking geometric context. The resulting atomization of form can generate apparently contradictory scaling patterns in what are, by definition, developmentally integrated morphologies. By contrast, landmark-based geometric morphometric analysis preserves spatial relationships,

permitting the simultaneous analysis of dimension and relative position, i.e., size and shape (Rohlf & Marcus, 1993). By relating geometrically derived shape variables to cranial size, it might be possible to identify global scaling patterns not discernable by traditional allometric analyses. Geometric analysis has the additional advantage of permitting direct visualization of shape trends—both allometric and nonallometric—in the original specimen space, thus facilitating description of results.

The present study applies geometric techniques to the description of allometric and size-uncorrelated cranial shape variation in adult papionins. Following Cheverud's (1982) demonstration that patterns of static adult allometry cannot be assumed to reflect ontogenetic processes, ontogenetic studies have come to be viewed as the allometric gold standard; however, it remains necessary to document patterns of adult interspecific allometry. Our understanding of the phylogenetic affinities of fossil papionins such as *Parapapio* and *Paradolichopithecus* (Szalay & Delson, 1979; Fleagle, 1999) could be significantly improved by interpretation within the context of papionin allometric shape variation. But, given the rarity of adequate fossil primate ontogenetic sequences, these forms can only be evaluated on the comparative basis of adult interspecific scaling patterns. To this end, this paper documents adult patterns of cranial shape variation in papionin primates, interprets these patterns in light of prior studies of papionin ontogeny and phylogeny, and considers their implications for the development and evolution of papionin cranial form.

Materials and methods

Data collection

The sample comprised 238 adult individuals from all six extant papionin genera (Table 1). The sample was largely limited to wild-shot adult individuals of known

Table 1 Study sample

Taxon	<i>n</i>		Collection*
	Female	Male	
<i>Cercocebus galeritus agilis</i>	10	7	AMNH
<i>Cercocebus torquatus torquatus</i>	6	13	AMNH PCM
<i>Lophocebus albigena johnstoni</i>	12	21	AMNH
<i>Macaca fascicularis</i>	17	26	AMNH UCMVZ
<i>Mandrillus leucophaeus</i>	8	19	BMNH FMNH FSM
<i>Mandrillus sphinx</i>	8	13	AMNH BMNH FSM PCM
<i>Papio hamadryas anubis</i>	21	41	AMNH FMNH NMNH UCMVZ
<i>Theropithecus gelada</i>	4	11	AMNH FMNH LHES NMNH

*Collection abbreviations: AMNH=American Museum of Natural History; BMNH=British Museum (Natural History); FMNH=Field Museum of Natural History; FSM=Senckenberg Natural History Museum—Frankfurt; LHES=Laboratory for Human Evolutionary Studies—UC Berkeley; PCM=Powell–Cotton Museum; NMNH=National Museum of Natural History; UCMVZ=University of California Museum of Vertebrate Zoology.

provenience. However, given the scarcity of *Theropithecus gelada* in museum collections, four zoo specimens (two male, two female) lacking obvious pathology and judged to present normal, “wild-type” morphology were included in the sample.

Data consisted of three-dimensional cranial landmarks recorded using a Microscribe 3-DX digitizer and *InScribe-32* software (Immersion Corp., San Jose, CA). This study was conducted in collaboration with the Morphometrics Research Group of the New York Consortium in Evolutionary Primatology, and cranial landmark data were collected by several observers under a common protocol developed by Frost *et al.* (in prep.). Each skull was first mounted to provide access to its dorsal aspect and osteometric landmarks recorded followed by four arbitrarily chosen, noncoplanar, noncollinear registration landmarks. The skull was then remounted to gain access to its ventral aspect and the remaining landmarks were recorded along with the same four registration landmarks. The registration landmarks were used to align the dorsal and ventral aspects of the skull within a common coordinate system, yielding a complete configuration. Realignment was performed on a

Silicon Graphics O₂ workstation using dedicated software combining *UNIX* and *Matlab 4.2c* routines (Frost *et al.*, in prep.). This dorsal–ventral landmark registration (DVLR) procedure allows all regions of the skull to be digitized without the use of cumbersome mounting equipment.

Following Frost *et al.* (in prep.), eleven midsagittal and 17 bilateral landmarks were recorded, yielding a maximum of 45 landmarks for each specimen (Figure 2, Table 2). At present, many geometric morphometric programs are unable to accommodate missing data. Where specimens are missing landmarks, whether due to antemortem pathology or postmortem damage, it is necessary either to exclude the specimen from analysis or to reconstruct the missing data. For specimens with localized damage, missing values for paired landmarks can be estimated by “reflecting” the corresponding landmarks from the opposite side to produce complete configurations. Specimens with missing data were read into *GRF-ND* (Slice, 1999) and Bookstein shape coordinates (Bookstein, 1991) were computed relative to an inion–prosthion baseline using bregma as the third landmark and invoking the “No Scale” option to preserve the original

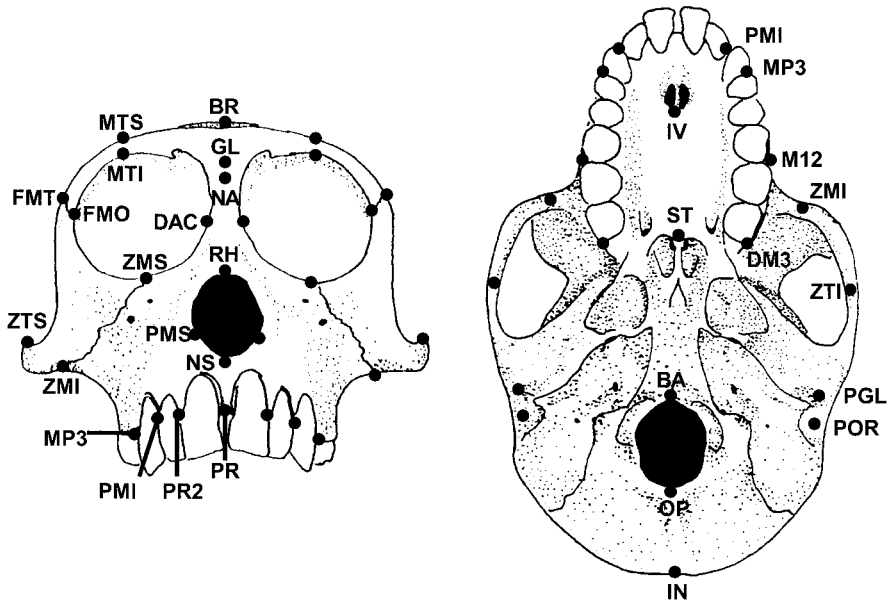


Figure 2. Osteological landmarks used in this study mapped on to a representative papionin skull (female *Macaca fascicularis*). Landmarks are defined following Frost *et al.* (in prep.); abbreviations follow Table 2. Line drawings of female *Macaca fascicularis* skull courtesy of J. Michael Plavcan (© J. M. Plavcan) and adapted with artist's permission.

specimen scale. This procedure oriented each specimen in a coordinate system with the Z-coordinate axis perpendicular to the specimen mid-sagittal plane and the origin located on the specimen midline at inion. Coordinates for each missing landmark were then taken from those of its antimere by reversing the sign of the Z-coordinate. The large number of specimens with damage in the region of Basion, an unpaired landmark, necessitated its exclusion, leaving a total of 44 landmarks for analysis.

Precision studies

Data used in this study were collected by three observers working under a common data collection protocol. To examine the effects of intra- and interobserver error, each observer collected multiple observations of a single specimen, a male *P. hamadryas ursinus* cranium. Raw landmark data were subjected to generalized Procrustes analysis (GPA) using GRF-ND (Slice, 1999) in order to

place all observations in a common frame of reference, and the Euclidean distance of each landmark to its respective centroid was computed. For each observer, landmark deviations were calculated relative to the observer landmark mean. Mean deviations and percentage errors were calculated for individual landmarks and subsequently averaged to give a mean deviation and percentage error for each observer across all landmarks (Table 3). One-way analysis of variance (ANOVA) was conducted for each landmark by observer, and the root mean squares were examined (Table 4). In the context of this analysis, the root of the within-groups mean squares (root mean square error) corresponds to intraobserver error (Sokal & Rohlf, 1981), while the root of between-groups mean squares corresponds to interobserver error. Intraobserver error does not exceed 0.33 mm or 2%. Interobserver error averages approximately 1 mm, again less than 2%, and even the

Table 2 Osteological landmarks

Landmark	Abbreviation
Midsagittal	
Inion	IN
Bregma	BR
Glabella	GL
Nasion	NA
Rhinion	RH
Nasospinale	NS
Prosthion	PR
Opisthion	OP
Basion	BA
Staphylion	ST
Incisivion	IV
Bilateral	
Prosthion-2	PR2
Mesial P ³	MP3
M ¹ -M ² Contact	M12
Distal M ³	DM3
Premaxillary suture-inferior	PMI
Premaxillary suture-superior	PMS
Zygomaxillare inferior	ZMI
Zygomaxillare superior	ZMS
Dacryon	DAC
Midtorus inferior	MTI
Midtorus superior	MTS
Frontomolare orbitale	FMO
Frontomolare temporale	FMT
Zygotemporale superior	ZTS
Zygotemporale inferior	ZTI
Porion	POR
Postglenion	PGL

Osteological landmarks used in the present study. Landmarks are defined following Frost *et al.* (in prep.) and are illustrated in Figure 2.

most imprecise observations do not exceed 5% error. While average interobserver error exceeds intraobserver error by approximately 0.66 mm, average percentage errors are comparable within and between observers. Given the relatively large size of the primate crania in this study, these margins of error were considered acceptable.

Procrustes analysis

Raw landmark data were subjected to a generalized Procrustes analysis (GPA) using the *Morpheus et al.* morphometrics package (Slice, 1998). GPA is an iterative least squares procedure in which individual

landmark configurations are scaled to unit centroid size and optimally superimposed so as to minimize summed squared distances across all landmarks and specimens relative to a reference configuration, the Procrustes mean (Slice *et al.*, 1996). Figure 3 shows the Procrustes superimposition of all 238 specimens in dorsal view. Differences between forms, indicated by the point scatters at each landmark, represent pure shape variation. It should be noted that, by scaling all specimens to unit centroid size, the Procrustes procedure corrects for gross size effects, i.e., scale, in a manner analogous to traditional bivariate ratios. But, as with ratios, Procrustes analysis *does not* correct for allometric effects. Therefore, the shape variation summarized by the Procrustes-aligned coordinates may include *both* size-correlated, i.e., allometric, and size-uncorrelated components.

Procrustes-aligned specimens may be represented as points in a curvilinear morphospace of dimension $3p-7$ for p three-dimensional landmarks (Dryden & Mardia, 1998; Rohlf, 1999a). Because this morphospace is non-Euclidean, statistical analysis is conducted using the orthogonal projection of points onto a Euclidean space set tangent to shape space at the Procrustes mean (Dryden & Mardia, 1998; Rohlf, 1999a). In practice, if shape variation is sufficiently small in the vicinity of the reference form, the Procrustes-aligned coordinates are a reasonable approximation of tangent space coordinates (Dryden & Mardia, 1998; Rohlf, 1999a). This assumption may be tested using *tpsSmall* (Rohlf, 1999b), software which computes the ordinary least squares regression (through the origin) of Euclidean (tangent space) distances versus the corresponding Procrustes (morphospace) distances for all possible specimen pairs. Analysis of the present data set showed a virtual one to one correspondence between the Procrustes and tangent spaces distances ($r=0.9999$, slope=0.9967)

Table 3 Observer mean deviation and mean percentage error across landmarks

Observer	<i>n</i>	Mean deviations			% Errors		
		Min	Max	Mean	Min	Max	Mean
1	10	0.07	0.54	0.24	0.07	1.00	0.42
2	8	0.06	0.55	0.16	0.06	1.04	0.26
3	6	0.05	1.42	0.25	0.07	1.77	0.40

Landmark mean deviations are computed as the mean of the absolute deviations of observations from the landmark mean [$ABS(x_i - \bar{x})$]; values are reported in millimeters. Landmark percentage error is calculated as the landmark deviation expressed as a percentage of the landmark mean [$ABS(x_i - \bar{x})/\bar{x}] \times 100$. Observer mean deviations and observer mean percentage errors are calculated as the mean value across all landmarks by observer.

Table 4 Inter- and intraobserver mean errors across landmarks

Level	RMSE			% RMSE		
	Min	Max	Mean	Min	Max	Mean
Intraobserver	0.10	1.10	0.31	0.10	1.47	0.51
Interobserver	0.04	2.81	1.05	0.32	4.70	1.70

Root mean square error (RMSE) is calculated as the root of the within-groups (intraobserver) or between-groups (interobserver) mean sums of squares for ANOVA of landmark distances by observer; values are reported in millimeters. Percentage root mean square errors (% RMSE) are calculated relative to the landmark grand mean as [$RMSE/\bar{X}] \times 100$. Mean RMSE and % errors are calculated as the mean value across all landmarks.

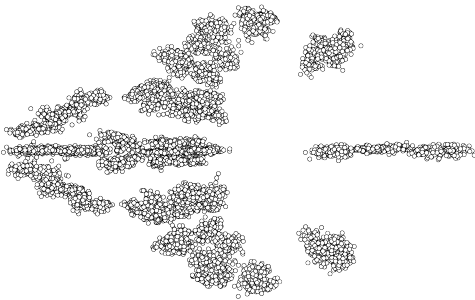


Figure 3. Dorsal view of Procrustes superimposition of 238 papionin crania. Specimens have been scaled to unit centroid size and optimally superimposed. In theory, all remaining differences between forms, indicated by point scatters at each landmark, are due to pure shape variation.

indicating that the Procrustes-aligned coordinates are a good approximation for tangent space coordinates.

Principal components analysis

Landmark-based morphometrics involves large numbers of statistically interdependent and partially redundant variables. Procrustes superimposition—through the constraints of translation, rotation, and unit scaling—results in the loss of additional degrees of freedom (Dryden & Mardia, 1998). Principal components analysis (PCA) of the Procrustes-aligned coordinates corrects for these spurious dimensions by reducing the data to a full-rank matrix, namely the principal component scores for axes corresponding to nonzero eigenvectors (Rohlf, 1999a). This procedure both generates a reduced number of statistically uncorrelated summary shape variables and ordines specimens relative to the major axes of shape variation (Dryden & Mardia,

Table 5 PCA of Procrustes-aligned coordinates

Component	Eigenvalue	Proportion	Cumulative
1	0.01090	0.667	0.667
2	0.00121	0.074	0.741
3	0.00088	0.054	0.794
4	0.00050	0.030	0.825
5	0.00040	0.024	0.849
6	0.00022	0.014	0.862
7	0.00018	0.011	0.874
8	0.00016	0.010	0.884
9	0.00014	0.009	0.892
10	0.00011	0.007	0.899

Principal Components 1–10 account for approximately 90% of total variance. Principal components 11 and higher each account for less than 1% of total variance.

1998). Principal components analysis was performed on the covariance matrix of the Procrustes-aligned coordinates using *SAS 6.12 for Windows* (SAS Institute, Cary, NC). Inspection of PCA results (Table 5) showed the first principal component to account for fully 67% of total shape variance. Cumulatively, the first ten principal components accounted for 90% of total variance, while the contributions of individual higher order components were negligible.

Because principal components analysis orients successive components in the direction of maximum variation (Neff & Marcus, 1980), a single divergent form can define the extremes of shape variation on multiple components, obscuring possible differences among the remaining taxa. Given the focus of this study on relationships among the mangabeys, baboons, and mandrills, the inclusion of *Theropithecus*, which exhibits a unique and highly derived cranial morphology (Szalay & Delson, 1979; Fleagle, 1999) was found to be counter-productive, and principal components were recomputed excluding *Theropithecus*. This had no effect on principal component ordinations, but it did result in a slight reordering of the principal component axes such that Principal Component 3, which

separates males and females within genera (see below), corresponds to Principal Component 5 of the initial analysis including all genera.

Regression analysis

To identify allometric effects, principal component scores were tested for significant linear relationships with size, represented here by cranial centroid size. Centroid size is defined as the square root of the sum of squared distances of a set of landmarks from their centroid (Slice *et al.*, 1996); computationally, it falls in the class of Mosimann size variables (Mosimann & Malley, 1979). Centroid size is the preferred size metric for Procrustes-based geometric morphometric analysis (Bookstein, 1996), both because it is the size measure upon which the computation of Procrustes distance is based and because it is approximately uncorrelated with all shape variables when assumptions of homogenous spherical landmark variance are met (Slice *et al.*, 1996). In the context of this study, cranial centroid size provides a reasonable estimate of cranial size and, given the scarcity of individual body mass data or associated postcrania, the best available surrogate for body size.

Principal component scores were plotted against log centroid size, Pearson product moment correlations were computed, and regression analyses were performed. As both dependent and independent variables were functions of landmark coordinates measured with error, a Type II regression analysis was performed (Sokal & Rohlf, 1981). Reduced major axis (RMA) regression equations were calculated and pairwise tests for homogeneity of slope and elevation were performed across genera using Cole's *NEWRMA* program (Cole, 1996). This program calculates Clark's (1980) test for homogeneity of slope and performs the nonparametric quick test for differences in elevation across all pairs of genera (Tsutakawa & Hewett, 1977). It also

generates bootstrap confidence intervals for between-group differences in slope and elevation at the sample grand mean.

Influential landmarks

In classic principal components analysis, influential variables are identified by inspection of eigenvectors, with large positive or negative coefficients indicating greater influence (Neff & Marcus, 1980). In three-dimensional morphometric studies, each landmark is represented by three variables, the X, Y, and Z coordinates, complicating the interpretation of eigenvectors and making it difficult to assess the influence of individual landmarks. To circumvent this difficulty, it was convenient to represent each landmark by a single variable. Thus, Procrustes-aligned coordinates were used to compute the Euclidean distance of each landmark to the common centroid. This yielded 44 distance variables, one per landmark, for each specimen. Principal components analysis was performed on the covariance matrix of these distance variables using *SAS 6.12 for Windows* (SAS Institute, Cary, NC). Principal components based on distances accounted for virtually identical proportions of the total shape variance and produced ordinations similar to those based on aligned coordinates. Having established the comparability of the two analyses, eigenvectors from the PCA of distances were examined. Inspection of eigenvectors showed coefficients in the range of ± 0.40 , with most landmark coefficients in the range of ± 0.15 . With few exceptions, paired landmarks showed coefficients of the same sign and similar magnitude, but values for paired landmarks (right and left) tended to diverge as the absolute magnitude of coefficients decreased. Based on this pattern, landmarks or landmark pairs with coefficient absolute values ≥ 0.15 were identified as influential for the component in question.

Visualization

Visualization of shape variation along selected principal component axes was performed using *Morphologika* (O'Higgins & Jones, 1999). Mean male and mean female configurations were computed for each taxon using backscaled Procrustes-aligned coordinates, thus summarizing average shape and size for each taxon. Mean forms were realigned and subjected to principal components analysis as above (O'Higgins & Jones, 1999). Inspection of the resulting principal component axes showed that principal component ordinations of mean forms corresponded closely to those based on individual specimens. The "Explore Shape Space" feature was then used to graphically explore shape variation along selected axes (O'Higgins & Jones, 1999). Shape variation along a principal component axis is visualized by adjusting the coordinates of the Procrustes mean form by the coefficients of the corresponding eigenvector. By generating a series of such forms, each corresponding to a different point along the axis, *Morphologika* can "morph" the mean form, displayed as a wireframe diagram, along an axis, thus visualizing shape variation summarized by that component (O'Higgins & Jones, 1999).

Canonical variates analysis

As an alternate approach to evaluating the size-uncorrelated component of papionin cranial shape variation, a canonical variates analysis was employed. Procrustes-aligned coordinates were regressed against log centroid size and the residual values, hereafter referred to as "size-adjusted coordinates", were subjected to canonical discriminant analysis using *SAS 6.12* (SAS Institute, Cary, NC). Mahalanobis distances were corrected for unequal sample sizes and the large number of variables using the formula for unbiased Mahalanobis distance of Marcus (1993). Similarly, significance levels for the Mahalanobis distances were adjusted

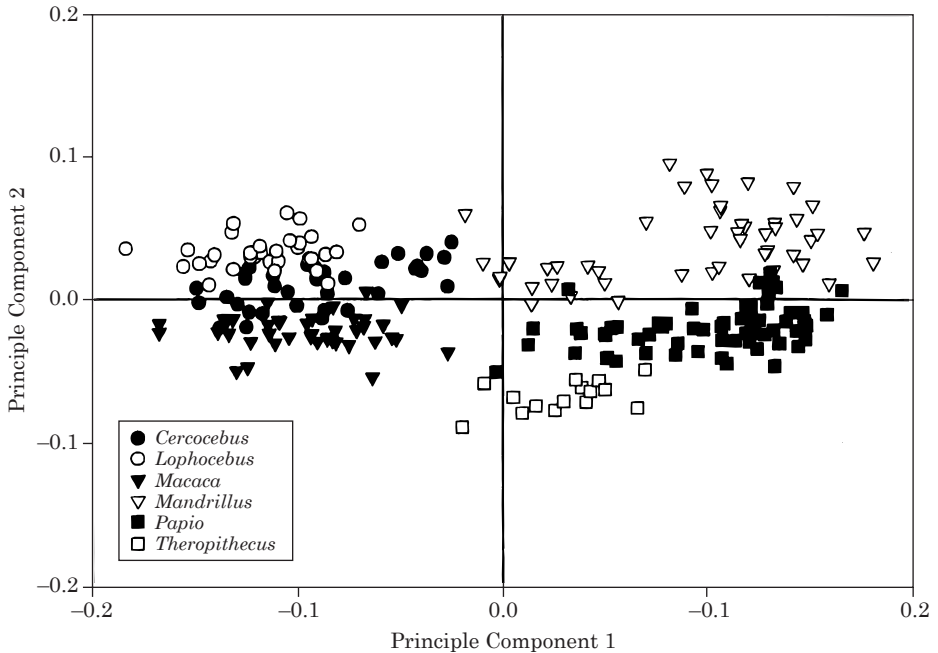


Figure 4. Plot of Principal Component 1 vs. Principal Component 2 based on PCA of Procrustes-aligned coordinate data. Principal Component 1 separates specimens into large-bodied and small-bodied groups, while Principal Component 2 distinguishes genera within the two size groups.

to account for multiple comparisons (Marcus, 1993). The resulting distance matrix was examined to assess the pattern and magnitude of inter-group distances and the canonical variates were plotted.

Results

Scaling relationships

The first principal component summarizes 67% of total shape variation and distinguishes large-bodied papionins—*Papio*, *Mandrillus*, and *Theropithecus*—from the smaller taxa (Figure 4). It is common in biological studies for the first principal component to be interpreted as “size” (Neff & Marcus, 1980); however, as previously noted, all specimens were scaled to unit size during the initial Procrustes analysis. Nevertheless, PC 1 clearly summarizes differences in shape between large- and small-bodied papionins, respectively.

Principal Component 1 was found to be highly significantly correlated with log centroid size across all papionins (Pearson’s $r=0.96$, $P<0.0001$), and Figure 5 demonstrates a strong linear relationship between these variables across genera. This implies that PC 1 largely summarizes size-correlated cranial shape variation and establishes that allometric scaling is present.

Table 6 shows coefficients for the reduced major axis regression of Principal Component 1 on log centroid size across all papionins and by genus. Within-genus relationships are weaker than those for the pooled sample, with r^2 values ranging from 0.68 for *Theropithecus* to 0.87 for *Papio*. Inspection of Figure 5 suggests that the pooled sample regression line is a reasonable estimator of genus slopes but not elevations. To test this impression, the pooled sample regression coefficients were treated as known values and compared to those for

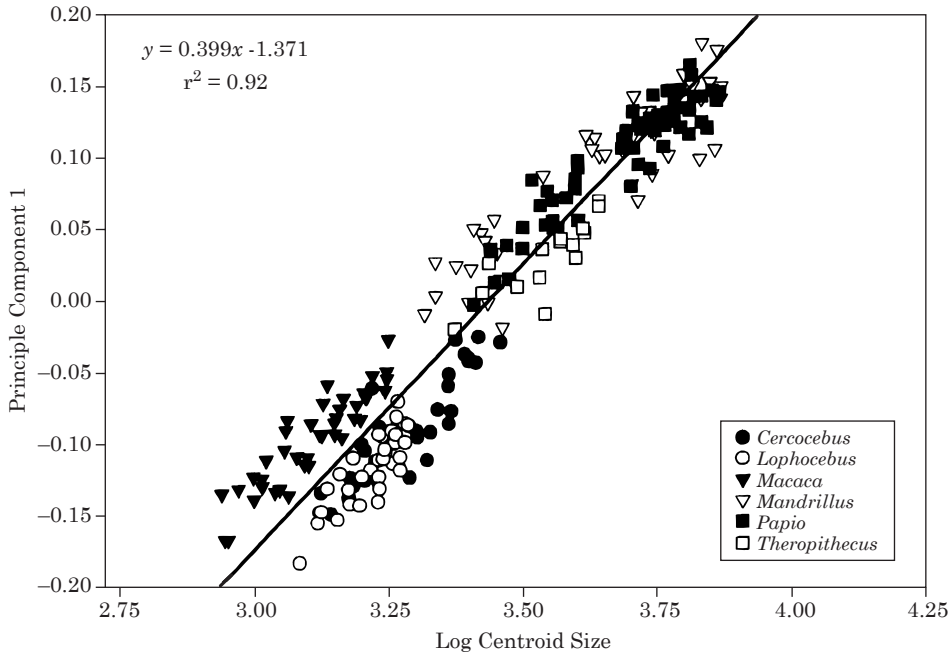


Figure 5. Reduced major axis regression of Principal Component 1 on log centroid size. The strong linear relationship between PC 1 and log centroid size confirms the presence of allometric scaling for aspects of cranial shape summarized by this component. There is considerable homogeneity of slopes among papionin genera but significant differences in elevation are observed.

Table 6 Reduced major axis regression coefficients for PC 1 on log centroid size across papionins and by genus

	Slope	95% CI†	Intercept	95% CI†	r ²
All Papionins	0.399	0.385 to 0.413	- 1.371	- 1.422 to - 1.321	0.918
<i>Cercocebus</i>	0.402	0.361 to 0.455	- 1.410*	- 1.584 to - 1.277	0.765
<i>Lophocebus</i>	0.470	0.390 to 0.549	- 1.628*	- 1.884 to - 1.372	0.702
<i>Macaca</i>	0.367	0.319 to 0.411	- 1.236*	- 1.376 to - 1.089	0.822
<i>Mandrillus</i>	0.317	0.280 to 0.549	- 1.062	- 1.210 to - 0.927	0.821
<i>Papio</i>	0.322	0.292 to 0.347	- 1.085	- 1.175 to - 0.974	0.872
<i>Theropithecus</i>	0.313	0.228 to 0.445	- 1.081	- 1.557 to - 0.776	0.682

Genus slopes are not significantly different from the pooled papionin slope using the single-sample test of Clarke (1980).

*Elevations significantly different from the pooled papionin line (Bonferroni adjusted $P=0.05$) using a modified quick test (Tsutakawa & Hewett, 1977) as follows: (1) under the null hypothesis that the genus elevation is equal to the pooled sample elevation, the prior probabilities of an individual case falling above or below the pooled regression line should be equal ($p=q=0.5$); (2) cases falling above and below the pooled sample line were tallied; and (3) the binomial probability of the resulting distribution was determined and the null hypothesis accepted or rejected accordingly.

†Bootstrap estimates of 95% confidence intervals generated by NEWRMA (Cole, 1996).

individual genera (see Table 6). Comparisons of individual genus slopes to that for the pooled sample found no statistically sig-

nificant differences from the common regression slope (Bonferroni adjusted $P=0.05$). In comparison with the pooled

Table 7 Pairwise comparisons of reduced major axis regression lines for PC 1 on log centroid size

	<i>Cercocebus</i>	<i>Lophocebus</i>	<i>Macaca</i>	<i>Mandrillus</i>	<i>Papio</i>	<i>Theropithecus</i>
<i>Cercocebus</i>	—	NS/NS	NS/†	NS/†	NS/†	NS/†
<i>Lophocebus</i>	NS/NS	—	NS/†	†/†	NS/†	NS/NS
<i>Macaca</i>	NS/*	*/*	—	NS/NS	NS/NS	NS/†
<i>Mandrillus</i>	*/*	*/*	NS/NS	—	NS/NS	NS/†
<i>Papio</i>	*/*	*/*	NS/NS	NS/NS	—	NS/†
<i>Theropithecus</i>	NS/NS	*/NS	NS/*	NS/*	NS/*	—

Results of Clarke's (1980) test for homogeneity of slope and the quick test for homogeneity of elevations (Tsutakawa & Hewett, 1977) are shown above the diagonal as slope/elevation, with significance levels adjusted for multiple comparisons. Results for bootstrap analysis (3000 replicates) of intergroup differences in slope and elevation at the pooled-sample grand mean are shown below the diagonal as slope/elevation; significance levels are not adjusted for simultaneous multiple comparisons. NS not significant at Bonferroni adjusted $P=0.05$; NS not significant at unadjusted $P=0.05$; †significant at Bonferroni adjusted $P=0.05$; *significant at unadjusted $P=0.05$.

sample line, *Cercocebus*, *Lophocebus*, and *Macaca* had highly significantly different elevations (Bonferroni adjusted $P < 0.001$), while the remaining taxa were not significantly different.

While the pooled sample regression line describes a general papionin allometric trend, pairwise testing of regression coefficients reveals statistically significant differences in scaling patterns between genera (Table 7). Four of the six papionin genera—*Macaca*, *Mandrillus*, *Papio* and *Theropithecus*—show a common slope for Principal Component 1 against log centroid size. *Macaca*, *Papio* and *Mandrillus* also share a common elevation from which *Theropithecus* may be offset. The slope for *Cercocebus* is intermediate between those of *Lophocebus* and *Macaca* and is not significantly different from either taxon; its elevation is likewise intermediate and indistinguishable from that of *Lophocebus* but differs significantly from *Macaca*. Results of slope comparisons between the mangabeys and the remaining papionin genera are contradictory. Under Clarke's test, only *Lophocebus* shows a significantly different slope from any other papionin genus, namely *Mandrillus*. Bootstrap estimates find both *Cercocebus* and *Lophocebus* to have significantly different slopes (unadjusted $P=0.05$) from the large-bodied taxa, *Papio*

and *Mandrillus*. Regression elevations for the mangabeys are clearly significantly different from those of *Papio* and *Mandrillus*. In summary, the papionins show substantial uniformity in the scaling of Principal Component 1 with respect to log centroid size overall, but both mangabey genera display significant differences in their scaling patterns from the remaining papionins.

Principal Components 2 and higher are, by definition, uncorrelated with PC 1 (Neff & Marcus, 1980), and were generally uncorrelated with size. Only PC 5 (analysis including *Theropithecus*) was significantly, albeit weakly, correlated with log centroid size ($r=0.16$, $P=0.01$); however, a bivariate plot of PC 5 against log centroid size (Figure 6) revealed linear relationships between these variables within genera and within-genus correlation coefficients greater than 0.5 (range 0.52–0.90). Principal Component 5 separates sexes within genera (see below), and the strongest correlations between PC 5 and size were observed in the most dimorphic genera. This could imply that PC 5 summarizes genus-specific allometric effects different from those summarized by PC 1. Unfortunately, in highly size-dimorphic taxa, any shape difference between the sexes will be correlated with size whether arising from allometric processes or not. Given the relative weakness of

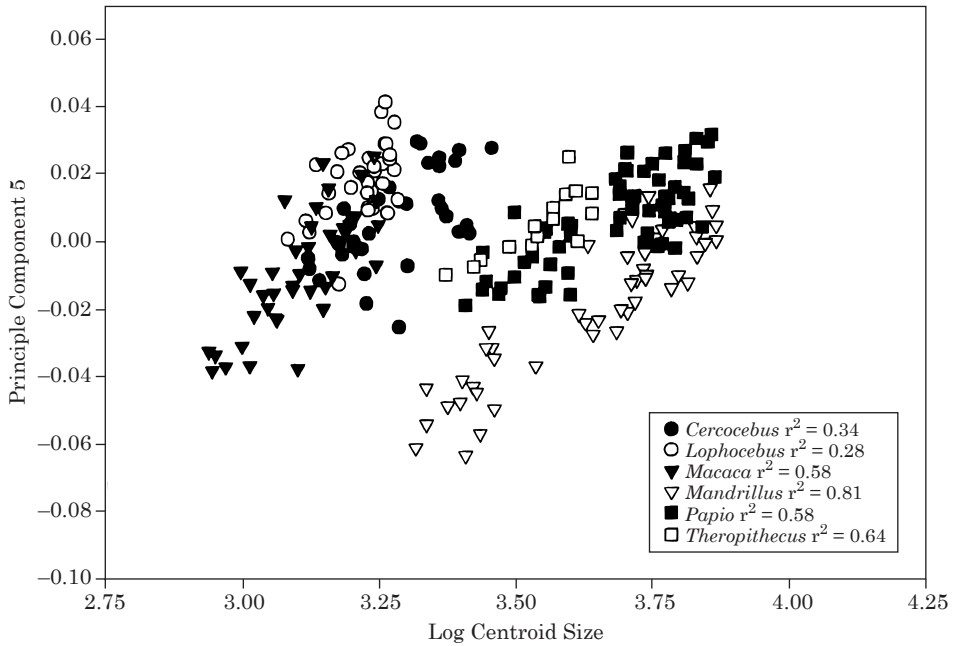


Figure 6. Plot of Principal Component 5 (analysis including *Theropithecus*) against log centroid size. PC 5 is significantly correlated with log centroid size within genera and separates males and females. As indicated by the r^2 values, this effect is more pronounced in the larger-bodied and most highly sexually dimorphic genera.

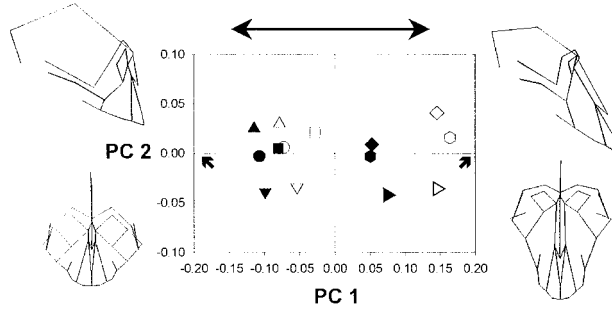
the observed correlations, it is likely that PC 5 incorporates both size-correlated and size-independent shape variation.

Because of concerns that within-taxon effects might influence interpretations of between-group shape variation, separate principal components analyses were conducted for males and females, respectively, and relationships of the resulting principal components with centroid size were examined. This procedure had the effect of generating higher-order principal components uncorrelated with centroid size, thus achieving a more rigorous statistical partition of shape variation into size-correlated and size-uncorrelated components. However, the resulting analyses produced principal component ordinations virtually identical to those for the combined-sex analysis. Between-genus comparisons of regression lines for PC 1 on centroid size were likewise

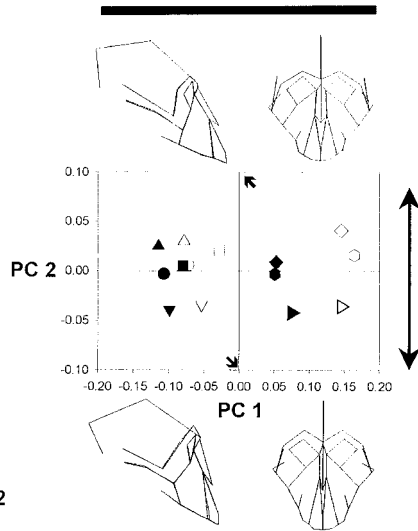
similar to the combined-sex analysis with only minor differences in significance levels, all easily attributable to the smaller single-sex sample sizes. In light of these results, it was concluded that single-sex analysis contributed nothing to the understanding of shape variation *among* genera and precluded the examination of sexual shape dimorphism *within* genera. Thus, results for combined-sex analyses are presented below.

Shape trends and influential landmarks

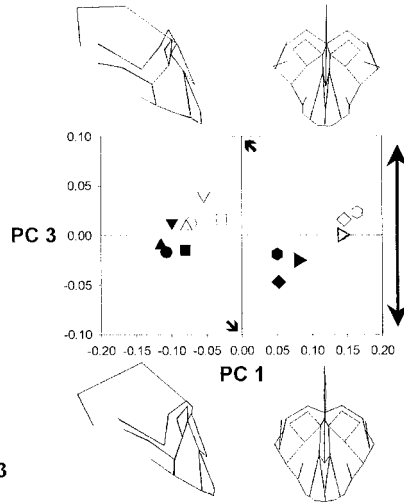
Figure 7 illustrates the shape differences summarized by Principal Components 1–5 (analysis excluding *Theropithecus*). It must be emphasized that, while shape trends along principal component axes frequently correspond with observed morphologies, they do not represent the actual physical appearance of specific animals. Rather, the wireframe diagrams illustrate morphometric



(a) PC 1

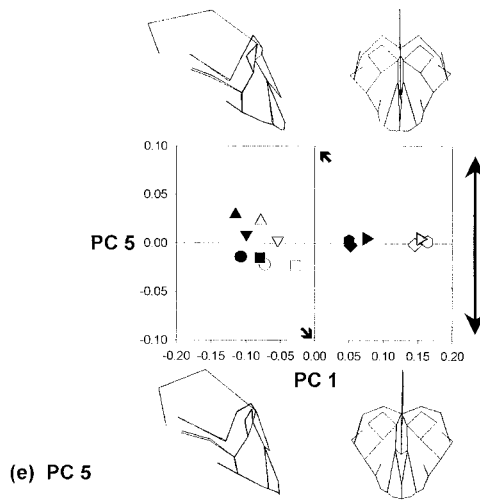
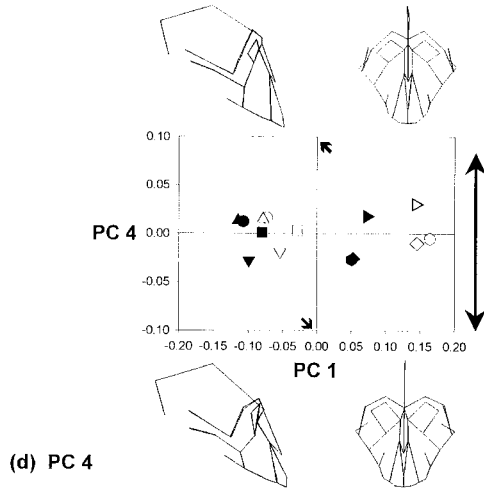


(b) PC 2



(c) PC 3

Figure 7. (a to c).



- *C. galeritus agilis* ♀
- *C. galeritus agilis* ♂
- *C. torquatus torquatus* ♀
- *C. torquatus torquatus* ♂
- ▲ *L. albigena johnstoni* ♀
- △ *L. albigena johnstoni* ♂
- ▼ *M. fascicularis* ♀
- ▽ *M. fascicularis* ♂
- ◆ *M. leucophaeus* ♀
- ◇ *M. leucophaeus* ♂
- *M. sphinx* ♀
- *M. sphinx* ♂
- ▶ *P. hamadryas anubis* ♀
- ▷ *P. hamadryas anubis* ♂

Figure 7. (d to f).

Table 8 Influential landmarks for Principal Components 1–5

PC	Positive coefficients	Negative coefficients
1	IN, BR, OP, PGL	RH, NS, PR, IV, PR2, MP3, PMI
2	GL, NA, DAC, MTI, MTS	IN, RH, OP, ST, IV, POR
3	IN, BR, GL, NA, OP, IV, PMS, DAC	FMT, ZTS, ZTI
4	IN, BR	ZMS, DAC
5	BR, ZMI, MP3	RH, PMS, MTS, ZTI

Influential landmarks and landmark pairs (right and left) are defined as those with absolute coefficients ≥ 0.15 for the principal component in question (see text). [Figure 8](#) maps influential landmarks for each component onto a representative papionin skull. Landmark abbreviations follow [Table 2](#).

trends along a subset of all possible axes of shape variation. In the following discussions, when a taxon is characterized as having a particular trait, it is always relative to all other taxa and with reference to the shape component in question. [Table 8](#) summarizes the influential landmarks which drive shape trends along Principal Components 1–5, and [Figure 8](#) displays the corresponding landmark maps.

As previously noted, the first principal component [[Figure 7\(a\)](#)] separates the papionin genera by size, with *Papio*, *Mandrillus*, and *Theropithecus* (where included) showing large positive scores, while *Cercocebus*, *Lophocebus*, and *Macaca* have negative scores. The large-bodied taxa are characterized by relatively small and low neurocrania; relatively small orbits and correspondingly short upper faces; and long, somewhat more dorsally oriented muzzles. Small-bodied taxa exhibit relatively large, globular neurocrania; large orbits and relatively tall upper faces; and shorter, more ventrally oriented muzzles. Consistent with this pattern, Principal Component 1 was found to be most strongly influenced by

landmarks of the neurocranium and anterior rostrum [[Figure 8\(a\)](#)]. It is tempting to construe this pattern as signifying “forward movement” of the anterior muzzle and “contraction” of the neurocranium, but it is ill-advised to give these landmark maps simple, mechanistic interpretations. Instead, each is best read conservatively as denoting regions of greatest morphological variation and, therefore, biological interest.

Principal Component 2 distinguishes *Macaca* and *Papio*, which exhibit relatively negative scores, from all other papionins [[Figure 7\(b\)](#)]. Visualizations show the former taxa to be relatively klinorhynch, showing prominence of the interorbital and supraorbital regions and a ventral deflection of the muzzle. By contrast, the remaining papionins show a more dorsally oriented face, producing a straighter profile and less projecting superior orbital margins. Principal Component 2 is influenced by rhinion and landmarks of the ventral neurocranium and palate, which show strong negative coefficients, with positively weighted landmarks in the interorbital region and along the supraorbital margins [[Figure 8\(b\)](#)].

Figure 7. Visualization of shape variation along Principal Components 1–5 (a)–(e). All plots show Principal Component 1 on the X-axis. Wireframe diagrams (frontal and lateral views) illustrate the extremes of shape variation summarized by a given axis (target axis indicated by double-headed arrow). These diagrams represent the transformation of the Procrustes mean form to the maximum and minimum axis values (indicated by single-headed arrows) with the other axis held constant at zero. Data points represent mean male and female forms for each taxon and indicate their positions relative to shape trends defined by each axis.

Principal Component 3 (analysis excluding *Theropithecus*) separates males, with relatively positive scores, from females, which exhibit relatively negative scores [Figure 7(c)]. This component corresponds to Principal Component 5 of the original analysis and is similarly correlated with log centroid size. Relative to conspecific males, females show more globular neurocrania, relatively larger orbits, a more parabolic palate outline, and narrow zygomatics. Males have lower neurocrania, relatively smaller orbits, a more parallel-sided palate, and flaring zygomatics. Principal Component 3 is most strongly influenced by landmarks of the neurocranium and inter-orbital and supraorbital regions, which show positive coefficients, with negatively weighted landmarks bracketing the zygomatics [Figure 8(c)].

Principal Component 4 distinguishes *Macaca* and female *Mandrillus* from *Papio*, with the remaining groups occupying intermediate positions along this axis [Figure 7(d)]. Visualizations show the former taxa to be characterized by relatively tall orbits and posteriorly positioned zygomatic roots. At the opposite extreme, *Papio* exhibits relatively short orbits, a deeper zygomatic, and anteriorly positioned zygomatic roots. Only four influential landmarks were identified for Principal Component 4, with inion and bregma having large positive coefficients and dacryon and zygomaxillare superior large negative coefficients [Figure 8(d)].

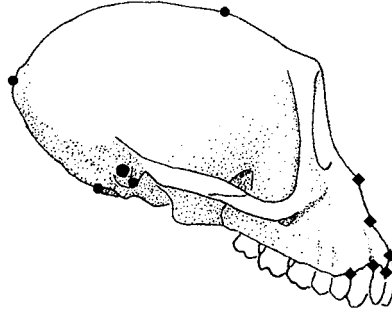
Principal Component 5 separates *Lophocebus* and *Cercocebus*, while all other taxa fall close to the origin. *Lophocebus* is characterized by a relatively low and long neurocranium; supraorbital margins high and arched; elongated and narrow nasals; a relatively narrow malar region; and a narrow palate [Figure 7(e)]. By contrast, *Cercocebus* shows a shorter and higher neurocranium; supraorbital margins low and relatively straight; shorter, broader nasals; a broader

malar region; and a broader and somewhat more parabolic palate. Principal Component 5 is most strongly influenced by bregma and landmarks bracketing the maxilla with positive coefficients, while landmarks of the anterior nasal region, supraorbital margin and zygomatic arch show negative coefficients [Figure 8(e)].

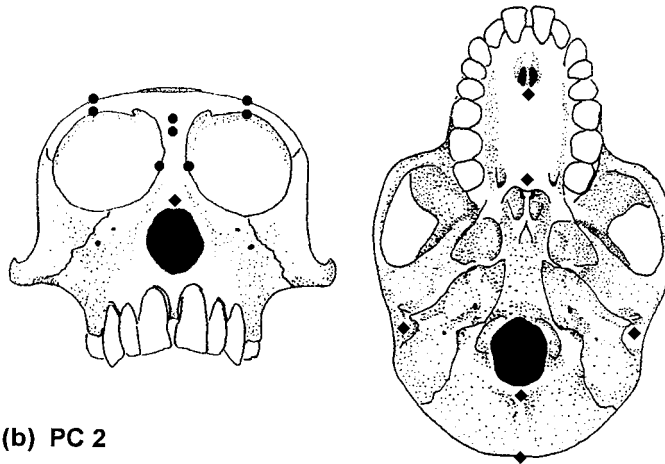
Canonical variates analysis

The first three canonical variates account for 56, 25 and 19% of total among-group variance, respectively for a cumulative total of over 99%. The fourth canonical variate, which separates males from females, accounts for less than 1% of total variance and is not statistically significant. Table 9 shows Mahalanobis distances between genera; all distances are highly significant (Bonferroni adjusted $P=0.001$). *Papio* consistently showed the smallest distances to other groups; *Lophocebus*, the largest. *Lophocebus* showed the smallest distance to *Papio*; *Cercocebus* was next closest to *Lophocebus*, followed by *Mandrillus*, and *Macaca*. *Cercocebus*, too, had its smallest distance to *Papio*, with *Mandrillus*, *Lophocebus*, and *Macaca* increasingly more distant. Similarly, *Macaca* and *Mandrillus* were each closest to *Papio*, and markedly more distant from the mangabeys. *Papio* was least distant from *Macaca* and farthest from *Lophocebus*. Notably, *Cercocebus* and *Lophocebus* are quite distant from each other, as are *Papio* and *Mandrillus*.

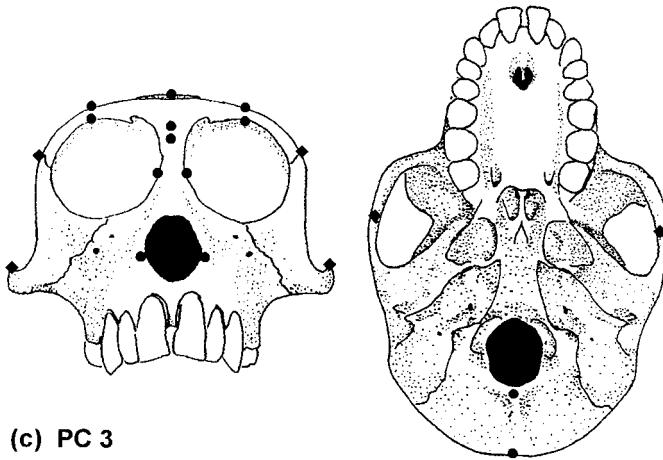
Figure 9 shows a three-dimensional plot of the first three canonical axes. Canonical Variate 1 separates *Macaca* from *Lophocebus*, with *Papio*, *Mandrillus*, and *Cercocebus* intermediate. Canonical Variate 2 contrasts *Papio* and *Mandrillus*. Canonical Variate 3 separates *Lophocebus* from *Cercocebus*. As might be predicted from the Mahalanobis distances, *Papio* and *Macaca* show the most similar pattern of residual shape variation with respect to the canonical axes. *Cercocebus* and *Mandrillus* show some similarities,



(a) PC 1

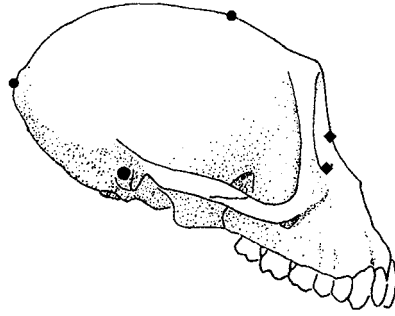


(b) PC 2

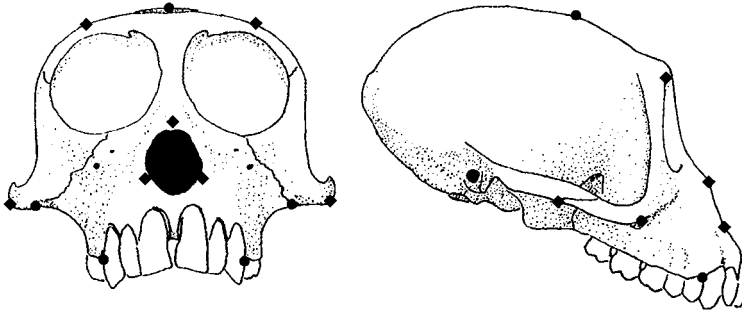


(c) PC 3

Figure 8. (a to c).



(d) PC 4



(e) PC 5

<ul style="list-style-type: none"> ● = Large Positive Coefficient ◆ = Large Negative Coefficient
--

Figure 8. (d and e).

Figure 8. Maps of influential landmarks for Principal Components 1–5 (a)–(e). Maps based on PCA of landmark distances (excluding *Theropithecus*). Influential landmarks (Table 8) are defined as those with absolute coefficients ≥ 0.15 for the principal component in question (see text). These landmarks identify regions of greatest morphological variability and contribute disproportionately to shape trends summarized by the corresponding principal component (see Figure 7). Line drawings of female *Macaca fascicularis* skull courtesy of J. Michael Plavcan (© J. M. Plavcan) and adapted with artist's permission.

both relative to the canonical axes and to *Papio*, but superimposition of a minimum spanning tree on the canonical clusters (not

shown) confirms that *Mandrillus* is most similar to *Macaca*. *Lophocebus* is widely separated from all other groups.

Table 9 Mahalanobis distances between papionin genera

	<i>Cercocebus</i>	<i>Lophocebus</i>	<i>Macaca</i>	<i>Mandrillus</i>	<i>Papio</i>
<i>Cercocebus</i>	—	16.64	20.99	15.00	14.07
<i>Lophocebus</i>	10.01	—	24.51	17.79	15.85
<i>Macaca</i>	12.85	15.07	—	13.45	11.60
<i>Mandrillus</i>	9.02	10.80	8.04	—	14.31
<i>Papio</i>	8.46	9.59	6.88	8.66	—

Mahalanobis distance values (D) are shown above the diagonal; unbiased Mahalanobis distance values (D_u)—corrected for unequal sample sizes and the large number of variables—are shown below the diagonal. All distances are significant at Bonferroni adjusted $P=0.001$. The unbiased squared Mahalanobis distance D_u^2 is computed as:

$$D_u^2 = \frac{D^2(N-g-p-1)}{(N-g)} \frac{(n_1+n_2)p}{n_1n_2}$$

where N =total sample size; g =number of groups; p =number of variables; and n_1 and n_2 are the sample sizes of the groups under comparison (Marcus, 1993).

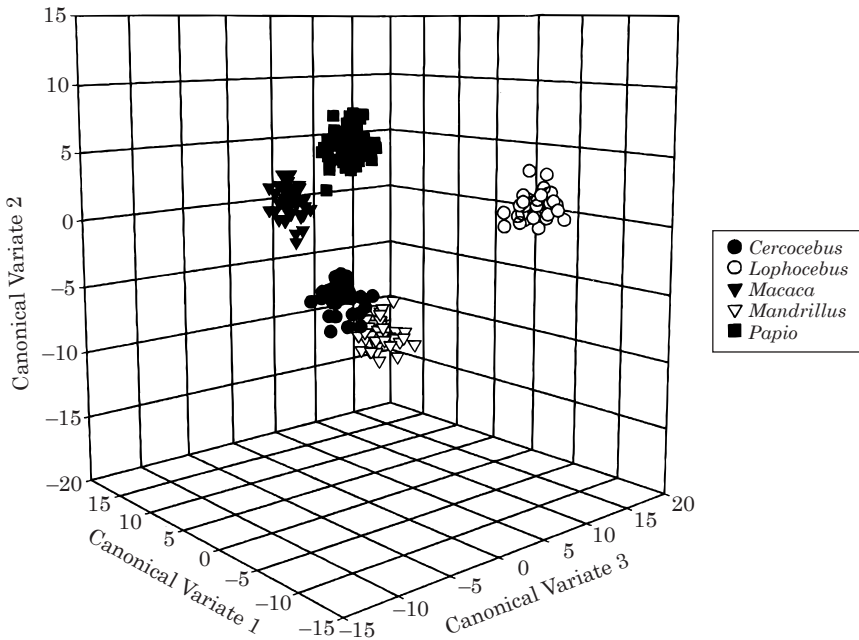


Figure 9. Three-dimensional canonical plot based on CVA analysis of size-adjusted landmark coordinates. *Macaca* and *Papio* show the most similar pattern of residual shape variation with respect to the canonical axes. *Lophocebus* is widely separated from all other taxa, including *Cercocebus*.

Discussion and conclusions

Combining geometric morphometric techniques and traditional bivariate and multivariate statistics, the present study takes

advantage of the complementary information these methods provide. Principal components analysis of aligned coordinate data serves the prosaic functions of data

reduction and ordination of specimens and permits a rough partition of total shape variation into size-correlated and size-uncorrelated moieties. Traditional regression analysis of morphometrically-derived size and shape variables simplifies the comparison of multivariate allometric relationships across and among groups, while Mahalanobis distances and canonical plots summarize patterns of overall morphological similarity when size effects are controlled. Direct visualization of shape components allows exploration of allometric shape trends and patterns of residual shape variation, while the corresponding landmark maps localize shape variation to specific regions of the skull.

Allometric effects

Principal Component 1, which summarizes 67% of total cranial shape variation, is highly significantly correlated with cranial size. Thus, craniofacial allometry is present in the Papionini; however the precise nature of scaling relationships among papionin taxa is complex. Parametric and nonparametric tests for homogeneity of slopes and intercepts produced broadly similar results, but inconsistencies were observed between different tests and significance levels were often borderline making some results inconclusive. Pairwise comparisons of regression coefficients showed that *Macaca*, *Papio*, *Mandrillus*, and *Theropithecus* share a common slope for PC 1 on log centroid size. *Macaca*, *Papio* and *Mandrillus* also share a common elevation, and thus fall on a common line from which *Theropithecus* may or may not be vertically transposed. In the latter case, results of the quick test and bootstrap were contradictory, due in part to the small sample size and relatively low r^2 values for *Theropithecus*. Larger samples will be required to adequately assess scaling patterns for this taxon. *Cercocebus* also shares the common papionin slope; however, its elevation differs from the large-bodied

animals and possibly *Macaca*. Results for *Lophocebus* are the most ambiguous. It clearly shares a common slope and elevation with *Cercocebus*. Like *Cercocebus*, it may also share a common slope with *Macaca*, *Papio*, and *Theropithecus*, but not *Mandrillus*. In any case, the mangabeys share a common scaling pattern to the exclusion of the remaining papionins.

Strictly defined, ontogenetic scaling occurs when observed differences in shape are “produced or accompanied by extension or truncation of common (or ancestral) growth allometries” (Shea, 1985:179). A finding that adults of closely related species share common allometric patterns is often indicative of the presence of ontogenetic scaling but never, in itself, conclusive. The present finding of a shared adult allometric scaling pattern for *Macaca* and *Papio* is wholly consistent with previous growth studies reporting ontogenetic scaling for these taxa (Swindler & Sirianni, 1973; Swindler *et al.*, 1973; Profant, 1995). The presence of the same allometric pattern in *Mandrillus* and possibly *Theropithecus* raises the possibility that the aspects of craniofacial shape summarized by Principal Component 1 have a common ontogenetic basis in all large-bodied papionins as well as macaques. Although similar adult interspecific scaling patterns may be produced by functional allometry (Jim Cheverud, personal communication), the prevalence of ontogenetic scaling among catarrhine primates renders it the most plausible explanation for the observed similarities among adult static allometries.

While cranial developmental patterns of *Macaca* and *Papio* have been intensively studied, ontogenetic trends among the remaining papionin taxa are less well established. Profant (1995) found that papionins, including mangabeys, conformed closely to ontogenetic trajectories established for *Macaca*. However, Shah & Leigh (1995) reported incongruent ontogenetic scaling

patterns among *Cercocebus*, *Papio*, and *Mandrillus*, and Collard & O'Higgins (2000, 2001) describe heterogeneity of multivariate growth vectors among African papionins. The present study finds significant differences in patterns of adult static allometry between the mangabeys and the large-bodied papionins in that *Cercocebus* and *Lophocebus* share a common allometric line which is vertically transposed from that of the remaining taxa. The divergence of adult scaling patterns in *Cercocebus* and *Lophocebus* is inconsistent with models invoking simple truncation of common growth vectors and argues against the presence of ontogenetic allometry, at least in its narrowest sense. This interpretation is supported by the work of Collard & O'Higgins (2001) who report that significant differences between the ontogenetic trajectories of mangabeys and large-bodied papionins are already present early in postnatal development.

The apparent absence of classic ontogenetic allometry notwithstanding, allometric scaling is a major determinant of papionin cranial shape variation. Principal Component 1 summarizes a substantial portion of total shape variation and is strongly linearly related with size across all papionins. Although the small-bodied taxa—*Macaca*, *Cercocebus*, and *Lophocebus*—are transposed above and below the common RMA line, genus slopes are not significantly different from the pooled slope. Despite observed heterogeneities among taxa, the pooled-sample regression line appears to be a good estimator of this general allometric trend. Visualization of the shape variation summarized by PC 1 shows positive facial allometry, characterized by increased facial prognathism, and negative neurocranial allometry as cranial size increases. The corresponding landmark map supports this finding, identifying landmarks on the neurocranium, premaxilla, anterior maxilla, and anterior nasals as exerting particular influence on this component.

These results are not surprising given the extensive literature documenting mammalian cranial scaling patterns in general, and primate cranial scaling in particular. Cranial allometry characterized by positive facial scaling and changes in facial orientation is observed across varying time-scales and taxonomic levels in mammalian groups as diverse as equids (Reeve & Murray, 1942; Radinsky, 1984); domestic canids (Weidenreich, 1941); New World anteaters (Reeve, 1939); carnivores (Radinsky, 1981); and titanotheres (Hersh, 1934). Within Primates, positive facial allometry is well documented and sufficiently common to be accepted as a general trend among non-human catarrhines (Biegert, 1963; Vogel, 1968; Ravosa & Profant, 2000). The ontogenetic basis of this pattern has been most intensively studied in the extant great apes. In gorillas, chimpanzees, and orang-utans, cranial growth is dominated by relatively rapid forward growth of the face accompanied by increased infraorbital facial depth, dorsal rotation of the alveolar process, and decreased basicranial flexion (Krogman, 1931a,b,c; Shea, 1983, 1985; Leutenegger & Masterson, 1989). Extension of these ontogenetic trajectories produces cranial sexual dimorphism within species and differences in cranial form between the African apes (Krogman, 1931a,b,c; Giles, 1956; Shea, 1983, 1985; Leutenegger & Masterson, 1989; O'Higgins *et al.*, 1990; O'Higgins & Dryden, 1993). Among cercopithecoids, Shea (1992) documented similar trends for cercopithecins, where ontogenetic allometry appears to explain the craniofacial proportions of *Miopithecus*, the smallest extant catarrhine.

Within Papionini, comparative longitudinal growth studies of *M. nemestrina* and *P. (hamadryas) cynocephalus* have also described facial ontogenies dominated by positive forward growth of the rostrum and dorsal rotation of the maxilla and palate

(Swindler & Sirianni, 1973; Swindler *et al.*, 1973; McNamara *et al.*, 1976). Differential growth along these shared ontogenetic trajectories contributes to the shape differences observed between macaques and baboons; differences among species and subspecies of *Papio* and *Macaca*; and sexual shape dimorphism within species (Zuckerman, 1926; Freedman, 1962, 1963; Albrecht, 1980; Bookstein, 1985; Cochard, 1985; Cheverud & Richtsmeier, 1986; Leigh & Cheverud, 1991; Ravosa, 1991; Richtsmeier *et al.*, 1993). In the present study, Principal Component 1 summarizes a pattern of static multivariate cranial allometry across adult papionins which closely resembles established patterns of catarrhine cranial ontogeny as well as general trends in mammalian cranial allometry. These broader trends, irrespective of their developmental origins, appear sufficient to account for much of the homoplasy in papionin cranial form.

If the pattern of cranial allometry within the Papionini is less than noteworthy, the extent to which allometric trends drive overall cranial shape variation is remarkable. Profant (1995) found that allometric effects accounted for 98% of cranial shape variation among *Macaca fascicularis*, *Macaca nemestrina*, and *Papio (hamadryas) cynocephalus*, taxa known to share a common scaling trajectory. Even allowing for a greater diversity of adult morphologies in the current sample; observed heterogeneities of scaling patterns among taxa; and the proportion of Principal Component 1 variance not attributable to cranial size, allometric effects still account for over 60% of total cranial shape variation. This is consistent with the results of Profant & Shea (1994), who found that allometric effects explained a preponderance of craniometric variation within the Cercopithecinae, with papionins showing steeper allometric trajectories than cercopithecins. These slope differences resulted in greater morphological diversification for papionins

over equivalent size ranges (Profant & Shea, 1994; Ravosa & Profant, 2000). It is this marked divergence of form that is reflected in traditional morphological classifications uniting taxa occupying the extremes of the papionin size ranges. An emphasis on cranial proportions in general, and relative facial length in particular, resulted in papionin phylogenies heavily influenced by size-correlated features.

Residual shape variation

Residual shape variation encompasses shape differences due to all factors other than allometry, including phylogenetic effects. Canonical discriminant analysis of size-adjusted coordinates and visual exploration of size-uncorrelated shape components provide complementary information about patterns of residual shape variation. The former summarizes overall morphological similarity, while the latter gives insights into patterns of cranial shape variation which contribute to these similarities.

The Mahalanobis distance matrix based on size-adjusted coordinates (Table 9) shows little correspondence to common conceptions of papionin cranial form or phylogenetic relationships. Although *Lophocebus* has its greatest similarity with *Papio*, the latter actually falls closest to *Macaca*. *Cercocebus*, too, has its strongest similarity with *Papio*, while *Mandrillus* is actually slightly closer to *Macaca*. In fact, the observed pattern of inter-genus distances implies considerable morphological conservatism in papionin cranial form. Interestingly, *Lophocebus* is the most distinct of the non-*Theropithecus* African papionins, consistently showing the greatest pairwise distances. The canonical plot (Figure 9) supports this interpretation. With respect to the first three canonical axes, *Macaca* and *Papio* are most similar, while *Lophocebus* is clearly divergent from the other taxa and widely separated from *Cercocebus*.

Visualization of shape variation along Principal Component 5 (analysis excluding *Theropithecus*), whose extremes are occupied by *Cercocebus* and *Lophocebus*, respectively, identifies the shape differences which contribute to the morphological distance between these taxa [Figure 7(e)]. In comparison with *Cercocebus*, *Lophocebus* displays a lower neurocranium; a narrower and more dorsally oriented muzzle with relatively projecting nasals; and a narrower malar region with less flaring zygomatic arches. This agrees with Groves (1978) description of the “stretched out” appearance of *Lophocebus* skulls. Groves (1978) also noted the relatively shorter and broader orbits of *Cercocebus*, which are reflected here in differences in supraorbital configuration along PC 5 [Figure 7(e)] and highlighted by the strong influence of the mid-torus superior landmark [Figure 8(e)]. Interestingly, the observed pattern of shape differences between *Cercocebus* and *Lophocebus* represents a reversal of the general papionin allometric trend. Larger papionins typically show lower and narrower neurocrania and narrower faces, but *Lophocebus* is smaller than *Cercocebus*, both in body mass and cranial centroid size.

The second principal component [Figure 7(b)] united *Macaca* and *Papio* to the exclusion of other papionins, a result congruent with the canonical variates analysis and small Mahalanobis distance between these taxa. Visualization of shape trends along PC 2 shows *Macaca* and *Papio* to be relatively klinorhynch, with projecting interorbital and supraorbital regions and procumbent (ventrally-deflected) faces relative to other taxa. Supporting this, influential landmarks are found on the basicranium, antero-inferior palate, infraorbital region, and supraorbital margins [Figure 8(b)]. Relative prominence of the supraorbital region is a discernable feature of both *Macaca* and *Papio*, and *Papio* has long been recognized as exhibiting pronounced facial procumbence (Zuckerman,

1926; Freedman, 1963), showing markedly greater “downward bending” of the face than *Mandrillus* (see illustrations in Hill, 1974; Maier, 2000). While this feature is not ordinarily associated with the relatively orthognathic macaques, in comparison with the similar-sized *Cercocebus*, and particularly *Lophocebus*, the macaque lower face is, in fact, more ventrally oriented. Thus, *Papio* and *Macaca* appear to share a common pattern of facial hafting when allometric effects are controlled.

Principal Component 3 (analysis excluding *Theropithecus*) separates males and females and is correlated with centroid size within genera. Shape variation along this axis is similar in some respects to trends along Principal Component 1, probably reflecting within-taxon allometric effects (see above). However, patterns of shape variation along PC 3 also highlight differences between sexes which are not directly attributable to differences in cranial centroid size [Figure 7(c)]. In particular, female neurocrania, when scaled to unit size, are higher and more globular than those of their male counterparts but not appreciably longer. Males exhibit a more parallel-sided palate, while females show a more parabolic palatal outline, a difference clearly related to canine sexual dimorphism. Finally, males exhibit comparatively broad and flaring zygomatics in comparison with females, possibly reflecting differences in the relative size and orientation of the temporalis and masseter muscles (Swindler & Wood, 1982).

Principal Component 4 separates *Macaca* and female *Mandrillus* from other papionins, most notably *Papio*. The canonical discriminant analysis likewise places *Mandrillus* slightly closer to *Macaca* than *Papio*. This component appears to summarize differences in the orientation of the zygomatic bodies and the relative contribution of the orbit to total facial height; however, these differences are extremely subtle. Reference

to a small comparative sample found that male and female *Macaca fascicularis* do resemble female *Mandrillus sphinx* in the features highlighted by PC 4. In both, the orbits constitute roughly half of total facial height and the zygomatic bodies are somewhat “swept back”, giving the midface a visor-like appearance. This contrasts with male (and to a lesser extent female) *Papio*, where the malar regions are more anteriorly oriented and the orbits contribute a smaller proportion of total facial height. In contrast to other components, which show strong agreement between shape component visualizations and landmark maps, only four influential landmarks were identified for Principal Component 4 [Figure 8(d)] and these showed no clear correspondence to visualized shape trends [Figure 7(d)]. Of all the shape components considered, the pattern of variation along this component is least robustly supported and its significance, if any, is unclear.

Conclusions

Observed patterns of cranial shape variation among the Papionini indicate that the evolution of cranial form within this group is less straightforward than previously thought. The presence of a common allometric scaling pattern in *Macaca*, *Papio*, *Mandrillus*, and perhaps *Theropithecus*, suggests that this is a shared feature and represents the primitive condition for African papionins. Outgroup comparisons will be required to determine whether this pattern is a derived feature for papionins or a retention from a more distant cercopithecine ancestor. The downward transposition of allometric trajectories in *Cercocebus* and *Lophocebus* indicates that mangabeys are similar in possessing enlarged neurocrania and reduced muzzles in comparison with comparably sized macaques, mandrills, and baboons. Given the current understanding of papionin phylogeny, this shared mangabey scaling pattern is most parsimoniously

interpreted as homoplastic and a product of parallel evolution. However, it must be noted that Collard & O’Higgins (2001), applying similar methods to a somewhat different dataset, have reached exactly the opposite conclusion concerning the polarity of papionin cranial allometries. Studies including additional taxa occupying the full range of papionin body sizes may help clarify the distribution and polarity of cranial scaling patterns, but detailed growth studies in *Cercocebus*, *Lophocebus*, and the smaller macaques will be required to isolate the developmental basis for and timing of the initial divergence of allometric trajectories in this group. At the same time, renewed attention should be given to identifying ecological and functional selective forces contributing to variation in allometric scaling patterns among papionin primates.

On first inspection, size-uncorrelated shape components are not particularly informative concerning phylogenetic relationships among African papionins. While the second principal component separates the outgroup *Macaca* and, interestingly, *Papio* from all other taxa, no component unites members of the African molecular clades. Similarly, canonical analysis of size-adjusted coordinates shows no particular affinity between clade members when size effects are controlled. Thus, analysis of size-uncorrelated shape variation gives no direct support to molecular phylogenies. The results are perhaps more significant for what is *not* observed. When size-correlated shape variation is factored out, the pervasive similarities which have driven traditional classifications disappear. No shape component simultaneously unites the two mangabeys, on the one hand, and baboons and mandrills, on the other. Rather, Principal Component 2 distinguishes *Papio* and *Macaca* from *Mandrillus* and the mangabeys and Principal Component 5 separates *Cercocebus* and *Lophocebus*. Similarly, both Mahalanobis distances and

canonical plots show *Cercocebus* and *Lophocebus* to be clearly separated in canonical space, while *Papio* has its strongest morphometric affinities with *Macaca*.

As in the case of size-correlated shape variation, *Macaca* and *Papio* share a common pattern of residual shape variation which is inferred to be the ancestral papionin condition. Further studies including cercopithecine outgroups are needed to determine whether this pattern is unique to the Papionini or part of a common cercopithecine heritage. The observed pattern of Mahalanobis distances suggests that *Papio* represents the primitive morphometric pattern for African papionins, from which other taxa have diverged to varying degrees. Although *Cercocebus* and *Mandrillus* show certain similarities in their overall pattern of variation with respect to the canonical axes, patterns of residual variation do not give clear support to molecular phylogenies of the Papionini. Rather, they describe a remarkable level of conservatism in cranial form among non-*Theropithecus* papionins, with individual taxa exhibiting relatively minor variations on a common morphometric theme.

The Papionini are often cited as a particularly striking example of morphological homoplasy (Disotell, 1996; Lockwood & Fleagle, 1999; Collard & Wood, 2000). The present study documents patterns of homoplastic similarity in papionin cranial shape due to allometric effects and provides some indication of the processes which may contribute to this similarity. However, this study raises as many questions as it answers. Results do not resolve the question of mangabey cranial homoplasy, but rather reframe it more narrowly in terms of parallel shifts in allometric scaling patterns. Ontogenetic studies will be required to explicate the developmental origins of variation in papionin allometric trajectories. The inference that *Papio* preserves the primitive morphometric pattern for African papionins

implies that similarities in mangabey facial form result from parallel evolution. However, broader taxonomic samples incorporating additional papionin taxa and multiple outgroups are needed to reconcile conflicting results (cf. Collard & O'Higgins, 2001) and more rigorously test hypotheses of polarity for the shape trends observed here. Analyses of residual (size-uncorrelated) shape variation reveal an absence of morphometric affinity between *Cercocebus* and *Lophocebus* when size effects are controlled, but this lack of quantitative resemblance is belied by similarities in key qualitative features. Thus, it will be necessary to clarify the definition, phylogenetic distribution, and functional significance of distinctive papionin traits, particularly the presence of excavated facial fossae and the development of maxillary ridges (McGraw & Fleagle, 2000), before the issue of papionin craniofacial homoplasy can finally be laid to rest. These uncertainties notwithstanding, the present study significantly increases our knowledge of patterns of craniometric variation in extant papionin primates. It is hoped these results will provide a more robust comparative framework within which to evaluate fossil papionin taxa and enhance our understanding of the evolutionary history of this fascinating group.

Summary

Geometric morphometric analysis of cranial landmark data shows that allometric scaling of cranial shape is present across all papionins and accounts for certain craniofacial similarities between like-sized members of separate clades. Comparisons of regression lines show considerable homogeneity of scaling among papionin genera; however, results give no support to hypotheses of uniquely shared allometric scaling patterns either within papionin clades or across all African papionins.

Rather, *Cercocebus* and *Lophocebus* show minor differences in slope and highly significant negative displacement of their allometric lines relative to other papionins. Nevertheless, allometric trends reflecting general patterns of mammalian cranial allometry appear to be a major determinant of papionin cranial shape variation, contributing considerably to the marked divergence of form which is reflected in traditional classifications of this group. Analysis of size-uncorrelated shape variation gives no clear support to molecular phylogenies, but highlights the absence of morphometric similarity between the mangabey genera when size effects are controlled. Patterns of allometric and residual shape variation suggest conservatism of non-*Theropithecus* papionin cranial form, with *Papio* appearing to demonstrate a primitive morphometric pattern from which other African papionins, most notably *Lophocebus*, have diverged. Outgroup comparisons with cercopithecine taxa will be required to determine whether these trends are unique to the Papionini or inherited from a more distant cercopithecine ancestor. Descriptions of craniometric variation among extant papionins are a necessary basis for assessments of morphological and phylogenetic affinities of fossil taxa, and the present study lays the groundwork for future studies of extinct papionins.

Acknowledgements

This work was conducted under the auspices of the Morphometrics Research Group of the New York Consortium in Evolutionary Primatology and supported by NSF Research & Training Grant # BIR 9602234 (NYCEP) and NSF Special Program Grant # ACI-9982351 (E. Delson, L. F. Marcus, D. P. Reddy, N. Tyson, and W. K. Barnett, Principal Investigators). I especially wish to thank Eric Delson for

his continued interest in and support of this work.

I am indebted to Steve Frost and Tony Tosi for their substantial contributions to the NYCEP-MRG primate cranial database, without which this research would not have been possible. I also wish to thank the Curators and Collections Managers of the following institutions: the American Museum of Natural History, Department of Mammalogy; the National Museum of Natural History, Department of Mammalogy; the Field Museum of Natural History, Division of Mammalogy; the British Museum of Natural History, Department of Zoology; the Powell-Cotton Museum; the Senckenberg Natural History Museum—Frankfurt; the Laboratory for Human Evolutionary Studies—University of California Berkeley; and the University of California Museum of Vertebrate Zoology.

I am deeply grateful to Les Marcus, David Reddy, Dennis Slice, and James Rohlf for their patient guidance as I ventured into the brave new world of geometric morphometrics. Thanks are also due to Tim Cole, Dennis Slice, Richard Smith, Bill Jungers, Mike Plavcan, and John Hunter for advice on technical and statistical matters, and to Jim Cheverud for his thoughtful discussion of allometry and the meaning of Cheverud (1982). I wish to thank Dennis Slice and Paul O'Higgins for making beta copies of their morphometrics packages available and Mike Plavcan for granting permission to adapt his illustration of the female *Macaca fascicularis* skull.

Steve Frost, Les Marcus, Mike Plavcan, Steve Leigh, and two anonymous reviewers provided comments on various drafts of this paper which improved the final product considerably. Any errors of fact or interpretation are, of course, my own.

This paper is NYCEP Morphometrics Contribution #3.

In Memoriam: This paper is dedicated to the memory of Leslie Marcus, whose

contributions to the field of geometric morphometrics were exceeded only by his generosity to his friends and colleagues.

References

- Albrecht, G. H. (1980). Longitudinal, taxonomic, sexual, and insular determinants of size variation in pigtail macaques, *Macaca nemestrina*. *Int. J. Primatol.* **1**, 141–152.
- Barnicot, N. A. & Hewett-Emmett, D. (1972). Red cell and serum proteins of *Cercocebus*, *Presbytis*, *Colobus* and certain other species. *Folia primatol.* **17**, 442–457.
- Biegert, J. (1963). The evaluation of characteristics of the skull, hands, and feet for primate taxonomy. In (S. L. Washburn, Ed.) *Classification and Human Evolution*, pp. 116–145. Chicago: Aldine Press.
- Bookstein, F. L. (1985). Modeling differences in cranial form, with examples from primates. In (W. L. Jungers, Ed.) *Size and Scaling in Primate Biology*, pp. 207–229. New York: Plenum Press.
- Bookstein, F. L. (1991). *Morphometric Tools for Landmark Data*. Cambridge: Cambridge University Press.
- Bookstein, F. L. (1996). Combining the tools of geometric morphometrics. In (L. F. Marcus, M. Corti, A. Loy, G. J. P. Naylor & D. E. Slice, Eds) *Advances in Morphometrics*, pp. 131–151. New York: Plenum Press.
- Burnett, G. T. (1828). Illustrations of the Manupeda or apes and their allies: being the arrangement of the Quadrumana or anthropomorphous beasts indicated in the outline. *Q. J. Sci. Lit. Art.* **26**, 300–307.
- Cheverud, J. M. (1982). Relationship among ontogenetic, static, and evolutionary allometry. *Am. J. phys. Anthropol.* **59**, 139–149.
- Cheverud, J. M. & Richtsmeier, J. T. (1986). Finite-element scaling applied to sexual dimorphism in rhesus macaque (*Macaca mulatta*) facial growth. *Syst. Zool.* **35**, 381–399.
- Clarke, M. R. B. (1980). The reduced major axis of a bivariate sample. *Biometrika* **67**, 441–446.
- Cochar, L. R. (1985). Ontogenetic allometry of the skull and dentition of the rhesus monkey (*Macaca mulatta*). In (W. L. Jungers, Ed.) *Size and Scaling in Primate Biology*, pp. 231–255. New York: Plenum Press.
- Cole, T. M. (1996). *NEWRMA*. Department of Basic Medical Sciences, University of Missouri, Kansas City, MO.
- Collard, M. & O'Higgins, P. (2000). Ontogeny and homoplasy in the papionin face. *Am. J. phys. Anthropol.* Suppl. **30**, 128.
- Collard, M. & O'Higgins, P. (2001). Ontogeny and homoplasy in the papionin monkey face. *Evol. Dev.* **3**, 322–331.
- Collard, M. & Wood, B. (2000). How reliable are human phylogenetic hypotheses? *Proc. natl. Acad. Sci. USA* **97**, 5003–5006.
- Cronin, J. E. & Sarich, V. M. (1976). Molecular evidence for dual origin of mangabeys among Old World primates. *Nature* **260**, 700–702.
- Delson, E. (1973). Fossil colobine monkeys of the Circum-Mediterranean region and the evolutionary history of the Cercopithecoidea. Ph.D. Dissertation, Columbia University.
- Delson, E. (1975a). Evolutionary history of the Cercopithecoidea. In (F. S. Szalay, Ed.) *Contributions to Primatology. Vol. 5: Approaches to Primate Paleobiology*, pp. 167–217. Basel: Karger.
- Delson, E. (1975b). Paleogeology and zoogeography of the Old World monkeys. In (R. Tuttle, Ed.) *Primate Functional Morphology and Evolution*, pp. 37–64. The Hague: Mouton.
- Delson, E. & Dean, D. (1993). Are *Papio baringensis* R. Leakey, 1969, and *P. quadratiostris* Iwamoto, 1982, species of *Papio* or *Theropithecus*? In (N. G. Jablonski, Ed.) *Theropithecus: The Rise and Fall of a Primate Genus*, pp. 125–156. Cambridge: Cambridge University Press.
- Delson, E., Terranova, C. J., Jungers, W. L., Sargis, E. J., Jablonski, N. G. & Dechow, P. C. (2000). Body mass in Cercopithecoidea (Primates, Mammalia): estimation and scaling in extinct and extant taxa. *Anthr. Papers Am. Mus. Nat. Hist.* **83**, 1–159.
- Disotell, T. R. (1994). Generic level relationships of the Papionini (Cercopithecoidea). *Am. J. phys. Anthropol.* **94**, 47–57.
- Disotell, T. R. (1996). The phylogeny of Old World monkeys. *Evol. Anthropol.* **5**, 18–24.
- Disotell, T. R., Honeycutt, R. L. & Ruvolo, M. (1992). Mitochondrial DNA phylogeny of the Old-World monkey tribe Papionini. *Mol. Biol. Evol.* **9**, 1–13.
- Dryden, I. L. & Mardia, K. V. (1998). *Statistical Shape Analysis*. New York: John Wiley.
- Dutrillaux, B., Fosse, A. M. & Chauvier, G. (1979). Étude cytogénétique de six espèces ou sous-espèces de mangabeys (Papiinae [sic], Cercopithecoidea). *Ann. Genet.* **22**, 88–92.
- Dutrillaux, B., Couturier, J., Muleris, M., Lombard, M. & Chauvier, G. (1982). Chromosomal phylogeny of forty-two species or subspecies of Cercopithecoidea (Primates, Catarrhini). *Ann. Genet.* **25**, 96–109.
- Fleagle, J. G. (1999). *Primate Adaptation and Evolution*. 2nd edn. New York: Academic Press.
- Fleagle, J. G. & McGraw, W. S. (1999). Skeletal and dental morphology supports diphyletic origin of baboons and mandrills. *Proc. natl. Acad. Sci. USA* **96**, 1157–1161.
- Freedman, L. (1962). Growth of muzzle length relative to calvaria length in *Papio*. *Growth* **26**, 117–128.
- Freedman, L. (1963). A biometric study of *Papio cynocephalus* skulls from northern Rhodesia and Nyasaland. *J. Mammalogy* **44**, 24–43.
- Frost, S. R., Marcus, L. F., Reddy, D. P., Bookstein, F. & Delson, E. (in prep.). Landmark comparison among large bodied papionins (Primates: Cercopithecoidea), with extension of procrustes methods to ridge curves.

- Groves, C. P. (1978). Phylogenetic and population systematics of the mangabeys (Primates: Cercopithecoidea). *Primates* **19**, 1–34.
- Groves, C. P. (2000). The phylogeny of the Cercopithecoidea. In (P. F. Whitehead & C. J. Jolly, Eds) *Old World Monkeys*, pp. 77–98. New York: Cambridge University Press.
- Harris, E. (2000). Molecular systematics of the Old World monkey tribe Papionini: analysis of the total available genetic sequences. *J. hum. Evol.* **38**, 235–256.
- Harris, E. & Disotell, T. R. (1998). Nuclear gene trees and the phylogenetic relationships of the mangabeys (Primates: Papionini). *Mol. Biol. Evol.* **15**, 892–900.
- Hewett-Emmett, D., Cook, C. N. & Barnicot, N. A. (1976). Old World monkey hemoglobins: deciphering phylogeny from complex patterns of molecular evolution. In (M. Goodman & R. E. Tashian, Eds) *Molecular Anthropology*, pp. 257–275. New York: Plenum Press.
- Hersh, A. H. (1934). Evolutionary relative growth in the titanotheres. *Am. Nat.* **68**, 537–561.
- Hill, W. C. O. (1974). *Primates: Comparative Anatomy and Taxonomy. Vol. 7: Catarrhini, Cercopithecinae, Cercocebus, Macaca, Cynopithecus*. Edinburgh: Edinburgh University Press.
- Jones, C. & Sabater Pi, J. (1968). Comparative ecology of *Cercocebus albigena* (Gray) and *Cercocebus torquatus* (Kerr) in Rio Muni, West Africa. *Folia primatol.* **9**, 99–113.
- Kingdon, J. (1997). *The Kingdon Field Guide to African Mammals*. San Diego: Academic Press.
- Krogman, W. M. (1931a). Studies in growth changes in the skull and face of anthropoids. III. Growth changes in the skull and face of the gorilla. *Am. J. Anat.* **47**, 89–115.
- Krogman, W. M. (1931b). Studies in growth changes in the skull and face of anthropoids. IV. Growth changes in the skull and face of the chimpanzee. *Am. J. Anat.* **47**, 325–342.
- Krogman, W. M. (1931c). Studies in growth changes in the skull and face of anthropoids. V. Growth changes in the skull and face of the orangutan. *Am. J. Anat.* **47**, 343–365.
- Kuhn, H.-J. (1967). Zur systematik der Cercopithecidae. In (D. Starck, R. Schneider & H.-J. Kuhn, Eds) *Neue Ergebnisse der Primatologie*, pp. 25–46. Stuttgart: G. Fischer.
- Leigh, S. R. & Cheverud, J. M. (1991). Sexual dimorphism in the baboon facial skeleton. *Am. J. phys. Anthropol.* **84**, 193–208.
- Leutenegger, W. & Masterson, T. J. (1989). The ontogeny of sexual dimorphism in the cranium of Bornean orang-utans (*Pongo pygmaeus pygmaeus*): II. Allometry and heterochrony. *Z. Morph. Anthropol.* **78**, 15–24.
- Lockwood, C. A. & Fleagle, J. G. (1999). The recognition and evaluation of homoplasy in primate and human evolution. *Yearb. phys. Anthropol.* **42**, 189–232.
- Maier, W. (2000). Ontogeny of the nasal capsule in cercopithecoids: a contribution to the comparative and evolutionary morphology of catarrhines. In (P. F. Whitehead & C. J. Jolly, Eds) *Old World Monkeys*, pp. 237–268. New York: Cambridge University Press.
- Marcus, L. F. (1993). Some aspects of multivariate statistics for morphometrics. In (L. F. Marcus, E. Bello & A. Garcia-Valdecasas, Eds) *Contributions to Morphometrics*, pp. 99–130. Madrid: Monografias Museo Nacional de Ciencias Naturales.
- McGraw, W. S. & Fleagle, J. G. (2000). Biogeography and evolution of the *Cercocebus*–*Mandrillus* clade. *Am. J. phys. Anthropol.* Suppl. **30**, 225.
- McNamara, J. A., Riolo, M. L. & Enlow, D. H. (1976). Growth of the maxillary complex in the rhesus monkey (*Macaca mulatta*). *Am. J. phys. Anthropol.* **44**, 15–26.
- Morales, J. C. & Melnick, D. J. (1998). Phylogenetic relationships of the macaques (Cercopithecidae: *Macaca*), as revealed by high resolution restriction site mapping of mitochondrial ribosomal genes. *J. hum. Evol.* **34**, 1–23.
- Mosimann, J. E. & Malley, J. D. (1979). Size and shape variables. In (L. Orioci, C. R. Rao & W. M. Stiteler, Eds) *Multivariate Methods in Ecological Work*, pp. 175–189. Fairland, MD: International Co-operative Publishing House.
- Nakatsukasa, M. (1994). Morphology of the humerus and femur in African mangabeys and guenons: functional adaptation and implications for the evolution of positional behavior. *Afr. Study Monographs Suppl.* **21**, 1–61.
- Nakatsukasa, M. (1996). Locomotor differentiation and different skeletal morphologies in mangabeys (*Lophocebus* and *Cercocebus*). *Folia primatol.* **66**, 15–24.
- Neff, N. A. & Marcus, L. F. (1980). *A Survey of Multivariate Methods for Systematics*. Numerical Methods in Systematic Mammalogy Workshop. American Society of Mammalogists.
- O'Higgins, P. & Dryden, I. L. (1993). Sexual dimorphism in hominoids: further studies of craniofacial shape differences in *Pan*, *Gorilla*, and *Pongo*. *J. hum. Evol.* **24**, 183–205.
- O'Higgins, P. & Jones, N. (1999). *Morphologika*. London: University College London.
- O'Higgins, P., Moore, W. J., Johnson, D. R. & McAndrew, T. J. (1990). Patterns of cranial sexual dimorphism in certain groups of extant hominoids. *J. Zool.* **222**, 399–420.
- Page, S. L., Chiu, C. & Goodman, M. (1999). Molecular phylogeny of Old World monkeys (Cercopithecidae) as inferred from γ -globin DNA sequences. *Mol. Phyl. Evol.* **13**, 348–359.
- Profant, L. (1995). Historical allometric inputs to interspecific patterns of craniofacial diversity in the cercopithecine tribe Papionini. *Am. J. phys. Anthropol.* Suppl. **20**, 175.
- Profant, L. & Shea, B. (1994). Allometric basis of morphological diversity in the Cercopithecini vs. Papionini tribes of Cercopithecine monkeys. *Am. J. phys. Anthropol.* Suppl. **18**, 162–163.
- Radinsky, L. (1981). Evolution of skull shape in carnivores. 1. Representative modern carnivores. *Biol. J. Linn. Soc.* **15**, 369–388.

- Radinsky, L. (1984). Ontogeny and phylogeny in horse skull evolution. *Evolution* **38**, 1–15.
- Ravosa, M. J. (1991). The ontogeny of cranial sexual dimorphism in two Old World monkeys: *Macaca fascicularis* (Cercopitheciinae) and *Nasalis larvatus* (Colobinae). *Int. J. Primatol.* **12**, 403–426.
- Ravosa, M. J. & Profant, L. P. (2000). Evolutionary morphology of the skull in Old World monkeys. In (P. F. Whitehead & C. J. Jolly, Eds) *Old World Monkeys*, pp. 237–268. New York: Cambridge University Press.
- Reeve, E. C. R. (1939). Relative growth in the snout of anteaters. A study in the application of quantitative methods to systematics. *Proc. Zool. Soc. Lond.*, Ser. A **110**, 47–80.
- Reeve, E. C. R. & Murray, P. D. F. (1942). Evolution in the horse's skull. *Nature* **150**, 402–403.
- Richtsmeier, J. T., Cheverud, J. M., Danahey, S. E., Corner, B. D. & Lele, S. (1993). Sexual dimorphism of ontogeny in the crab-eating macaque (*Macaca fascicularis*). *J. hum. Evol.* **25**, 1–30.
- Rohlf, F. J. (1999a). Shape statistics: Procrustes superimpositions and tangent spaces. *J. Classif.* **16**, 197–223.
- Rohlf, F. J. (1999b). *tpsSmall* v. 1.17. Department of Ecology and Evolution, State University of New York, Stony Brook, New York.
- Rohlf, F. J. & Marcus, L. (1993). A revolution in morphometrics. *Trends Evol. Ecol.* **8**, 129–132.
- Schwarz, E. (1928). The species of the genus *Cercocebus*. *Ann. Mag. Nat. Hist.* **5**, 664–670.
- Shah, N. F. & Leigh, S. R. (1995). Cranial ontogeny in three papionin genera. *Am. J. phys. Anthropol. Suppl.* **20**, 194.
- Shea, B. T. (1983). Allometry and heterochrony in the African apes. *Am. J. phys. Anthropol.* **62**, 275–289.
- Shea, B. T. (1985). Ontogenetic allometry and scaling: a discussion based on the growth and form of the skull in African apes. In (W. L. Jungers, Ed.) *Size and Scaling in Primate Biology*, pp. 175–205. New York: Plenum Press.
- Shea, B. T. (1992). Ontogenetic scaling skeletal proportions in the talapoin monkey. *J. hum. Evol.* **23**, 283–307.
- Slice, D. E. (1998). *Morpheus et al.: Software for Morphometric Research*. Revision 01-30-98. Department of Ecology and Evolution, State University of New York, Stony Brook, New York.
- Slice, D. E. (1999). *GRF-ND: Generalized Rotational Fitting of n-Dimensional Landmark Data*. Revision 12-15-99. Department of Ecology and Evolution, State University of New York, Stony Brook, New York.
- Slice, D. E., Bookstein, F. L., Marcus, L. F. & Rohlf, F. J. (1996). Appendix I—a glossary for geometric morphometrics. In (L. F. Marcus, M. Corti, A. Loy, G. J. P. Naylor & D. E. Slice, Eds) *Advances in Morphometrics*, pp. 531–551. New York: Plenum Press.
- Sokal, R. S. & Rohlf, F. J. (1981). *Biometry*. 2nd edn. New York: W. H. Freeman.
- Strasser, E. & Delson, E. (1987). Cladistic analysis of cercopithecoid relationships. *J. hum. Evol.* **16**, 81–99.
- Swindler, D. R. & Sirianni, J. E. (1973). Palatal growth rates in *Macaca nemestrina* and *Papio cynocephalus*. *Am. J. phys. Anthropol.* **38**, 83–92.
- Swindler, D. R. & Wood, C. D. (1982). *An Atlas of Primate Gross Anatomy: Baboon, Chimpanzee, and Man*. Malabar, FL: Krieger Publishing.
- Swindler, D. R., Sirianni, J. E. & Tarrant, L. H. (1973). A longitudinal study of cephalofacial growth in *Papio cynocephalus* and *Macaca nemestrina* from three months to three years. In *Symp. IVth Int. Congr. Primat. vol. 3: Craniofacial Biology of the Primates*, pp. 227–240. Basel: Karger.
- Szalay, F. S. & Delson, E. (1979). *Evolutionary History of the Primates*. New York: Academic Press.
- Thorington, R. W. & Groves, C. P. (1970). An annotated classification of the Cercopithecoidea. In (J. R. Napier & P. H. Napier, Eds) *Old World Monkeys—Evolution, Systematics, and Behavior*, pp. 629–648. New York: Academic Press.
- Tsutakawa, R. K. & Hewett, J. E. (1977). Quick test for comparing two populations with bivariate data. *Biometrics* **33**, 215–219.
- Van Der Kuyl, A. C., Kuiken, C. L., Dekker, J. T., Perizonius, W. R. K. & Goudsmit, J. (1995). Phylogeny of African monkeys based upon mitochondrial 12S rRNA sequences. *J. molec. Evol.* **40**, 173–180.
- Vogel, C. (1968). The phylogenetical evaluation of some characters and some morphological trends in the evolution of the skull in catarrhine primates. In (A. B. Chiarelli, Ed.) *Taxonomy and Phylogeny of Old World Primates with References to the Origin of Man*, pp. 21–55. Torino: Rosenberg & Sellier.
- Weidenreich, F. (1941). The brain and its role in the phylogenetic transformation of the human skull. *Trans. Am. Phil. Soc. N.S.* **31**, 321–442.
- Zuckerman, S. (1926). Growth-changes in the skull of the baboon, *Papio porcarius*. *Proc. Zool. Soc. Lond.* **55**, 843–873.